ORNL-TM-2732

Contract No. W-7405-eng-26

NASA Order No. C-90089-A
(Interagency Agreement 40-100-66)

FILLING HEAT STORAGE TUBES FOR SOLAR BRAYTON-CYCLE HEAT RECEIVER WITH LITHIUM FLUORIDE

P. A. Gnadt

JULY 1970

OAK RIDGE NATIONAL LABORATORY
Oak Ridge, Tennessee
operated by
UNION CARBIDE CORPORATION
for the
U.S. ATOMIC ENERGY COMMISSION

CONTENTS

FOREWORD AND ACKNOWLEDGMENTS

This report presents information on the design, fabrication, and operation of a facility to introduce lithium fluoride into columbium-1% zirconium heat storage tubes for a NASA solar Brayton-cycle heat receiver. The work was performed over a 30-month period under NASA Order C-90089-A and AEC Interagency Agreement 40-100-66 for the Space Power Systems Division, Lewis Research Center, National Aeronautics and Space Administration, under the technical supervision of Harry M. Cameron.

The contributions of many individuals during the design, fabrication, and operation of this facility were invaluable. In particular, acknowledgment is made of the metallurgical guidance and analysis received from B. Fleischer; and the efforts of E. J. Breeding, C. W. Collins, L. C. Fuller, and R. D. Stulting in mechanical and electrical design. Purification of the lithium fluoride and the salt analyses were accomplished under the direction of J. H. Shaffer. L. C. Fuller and J. H. Shaffer contributed to sections of this report concerning heat transfer and purification of lithium fluoride, respectively.

The author also wishes to acknowledge the guidance and technical assistance of R. E. MacPherson and A. J. Miller in the performance of this work.

FILLING HEAT STORAGE TUBES FOR SOLAR BRAYTON-CYCLE HEAT RECEIVER WITH LITHIUM FLUORIDE

P. A. Gnadt

Abstract

A facility was designed, fabricated, and operated to fill columbium-1% zirconium tubes with liquid lithium fluoride. Sixty-nine heat storage tubes were processed for a solar heat receiver that is a major component for a NASA solar-heated Brayton-cycle power unit. This 2- to 15-kw(e) dynamic power conversion system will eventually be used for earth orbit application. The lithium fluoride will provide heat storage capability for the shadow portion of the orbit. The salt-filled heat storage tubes described here were prepared for a prototype system to be tested in the NASA Plumbrook Facility by using a solar simulator.

The lithium fluoride was introduced into the annulus between a bellows-like outer tube and an inner gas duct that will carry the Brayton-cycle working fluid, a helium-xenon mixture (mol. wt = 84). The 48 columbium-1% zirconium tubes required for the actual system were filled with the molten salt, as well as eleven spares, six heat transfer test specimens, three thermal-cycling test specimens, and one preliminary test piece. The process required the use of a 120-ft^3 10-ft-high vacuum chamber, refractory metal jigs and fixtures, highly purified lithium fluoride at temperatures up to 1750°F, and much of the sophisticated technology the Oak Ridge National Laboratory has developed for the handling of high-melting-point salts (LiF m.p. = 1560°F).

Keywords: solar-heated Brayton cycle, space auxiliary power plant, heat storage tubes, lithium fluoride, columbium-1% zirconium alloy, molten salt, refractory metal.

Introduction

The Lewis Research Center of the National Aeronautics and Space Administration is developing a 10-kw solar-heated dynamic power conversion system.[1] This system incorporates the solar heat receiver shown in mockup in Fig. 1. This heat exchanger accepts radiant energy from a solar mirror and transmits the energy in the form of heat to the system's working fluid, a helium-xenon mixture (mol. wt = 84). Lithium fluoride contained in 48 convoluted (bellows configuration) tubes

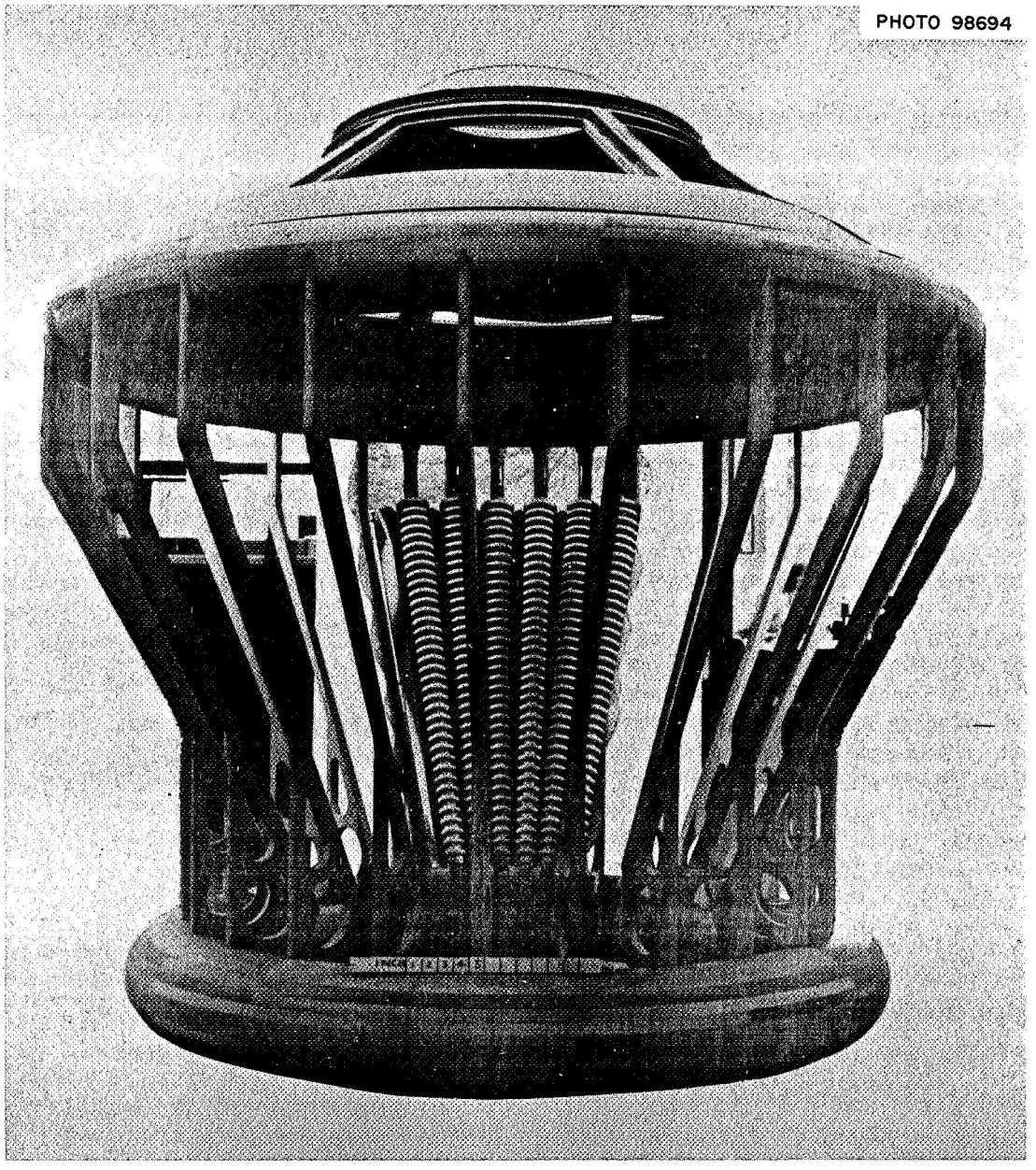

Fig. 1. Model of Brayton-Cycle Heat Receiver Designed by NASA Lewis Research Center.

(Fig. 2) stores heat, primarily by a solid-to-liquid phase change, during that portion of the orbit in which the system intercepts solar radiation. During the ecliptic portion of the orbit, the stored energy is utilized, and the salt is refrozen. The operating temperature range of the lithium fluoride is from 1500°F (60°F below the melting point) to 1750°F, a maximum hot-spot condition.

A prototype receiver is to be tested with other components of the solar Brayton-cycle system in the NASA Plumbrook Facility. The tubes for the receiver assembly were fabricated at the NASA-Lewis Research Center, and the detailed design, fabrication, and assembly of the receiver unit are to be accomplished at the General Electric Company's Nuclear System's Program facility at Evendale, Ohio. The Oak Ridge National Laboratory's participation in this program comprised filling the individual heat storage tubes with lithium fluoride.

This report describes the design and the equipment required for filling these tubes, the procedures used to fill 69 tubes with fused lithium fluoride, and the method of purifying the lithium fluoride.

Equipment Design Requirements

Design to Accommodate Lithium Fluoride Volumetric Expansion

The approximately 30% volumetric expansion that lithium fluoride undergoes at its melting point (1560°F), coupled with the differential thermal expansion characteristics of the molten salt and the columbium–1% zirconium tubes, introduced many special design and handling requirements. The prototype solar heat receiver is scheduled to operate with a maximum hot-spot temperature of 1750°F. Therefore it was necessary to preheat both the heat storage tubes and the lithium fluoride to this temperature and conduct the filling operation at this temperature to assure that excessive hydraulic pressures would not occur under the hot-spot condition. It also was considered necessary (again, to protect against excessive hydraulic pressure) that the filling and cooling operations provide each convolution of the heat storage tube with a lithium fluoride inventory equivalent to its volume at 1750°F. Further, it was

PHOTO 75228A

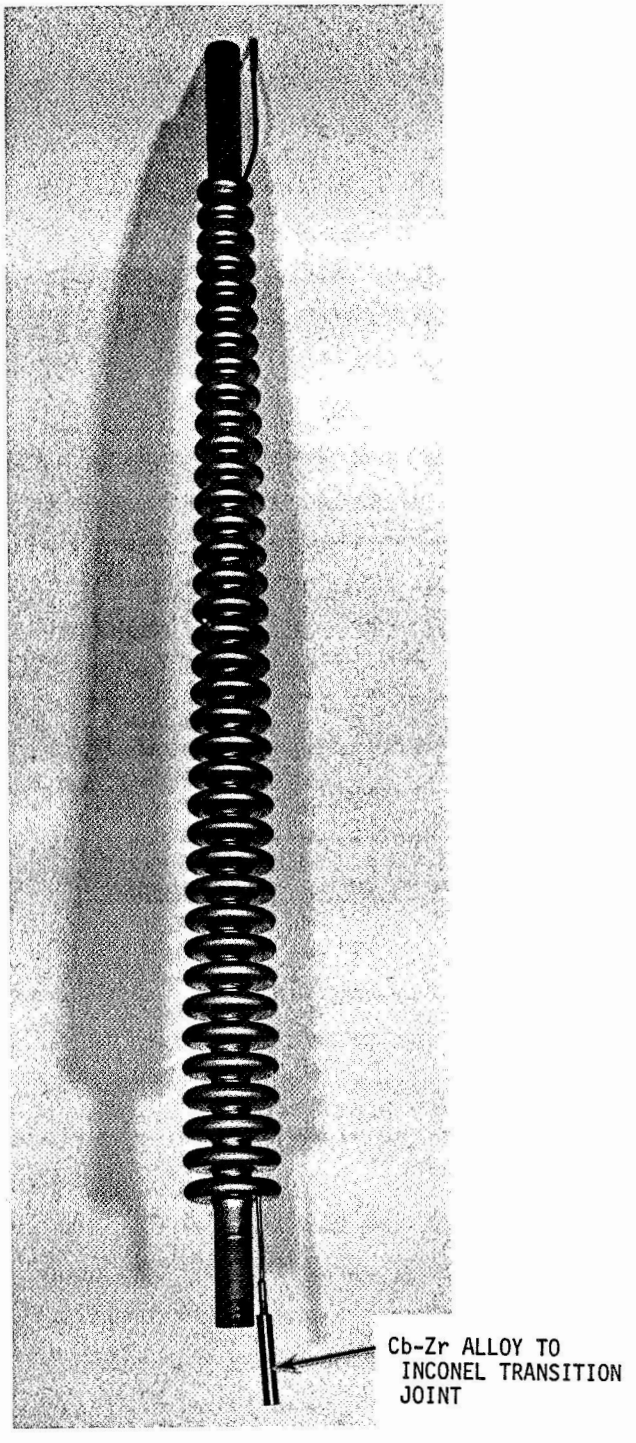

Fig. 2. Brayton-Cycle Heat Storage Tube.

essential that the lithium fluoride not run out into voids created by freezing the transfer lines and that it freeze and contract in the individual convolutions so that no transfer to or from adjacent convolutions could occur.

Freezing the lithium fluoride inventory of each bellows convolution in a predicable, uniform manner was accomplished by a combination of (1) forced cooling of the filled volume from the center of each tube to form a freeze plug at the bottom of each bellows convolution and (2) radiation from the outside of the bellows convolution. This method of cooling trapped the contents of each convolution and created a void volume in the center of each salt pocket. This void volume will accommodate the approximately 30% volumetric expansion of the lithium fluoride during the remelting cycle of heat receiver operation.

Design to Protect Heat Storage Tubes from Exposure to Oxygen

The susceptibility of the columbium–1% zirconium alloy to oxygen contamination at elevated temperatures and the subsequent embrittlement problem dictated that the filling operation be accomplished in a vacuum chamber. For this purpose, the heat storage tube assembly was installed in an existing vacuum chamber facility that provided a 4-ft-diam 10-ft-high diffusion-pumped volume. Consideration was given to location of the lithium fluoride reservoir and auxiliary equipment inside the chamber and the use of a single material of construction (columbium–1% zirconium alloy) to avoid vacuum chamber penetrations and dissimilar metal joints. However, the chamber would not accommodate all the required equipment, and sufficient refractory material was not readily available. In addition almost completely remote operation would have been necessary. Therefore the filling equipment was fabricated from Hastelloy N and Inconel 600.

Development of Brazed Joints

The use of nickel-base alloys in part of the system dictated the use of transition joints wherever these alloys were to be joined to the columbium–1% zirconium material. Commercial transition joints were

available; however, approximately 75 joints were required for the job, and it was not economically feasible to use the commercial joints. The ORNL Metals and Ceramics Division developed and tested a brazed joint that was adequate for use during the filling operation. The cost of these joints, including the development and testing operations, was approximately 10% of the cost of the commercially available joints. The successful development of the transition joint permitted a design in which the columbium–1% zirconium material was in the vacuum chamber and the nickel-base alloys were outside the chamber.

Specifications for Materials, Welding, and Inspection

Nickel-base alloy material specifications, welding, and inspection were in accordance with ORNL Metals and Ceramics Division specifications. The columbium–1% zirconium material for the assembly fixture and transition joints was, in general, procured from surplus material stock originally purchased at the CANEL Facility, Middletown, Connecticut, which is operated by Pratt & Whitney Aircraft Company. The welding of columbium–1% zirconium material was in accordance with special procedures developed by the ORNL Metals and Ceramics Division and the Y-12 Plant Production Division of the Union Carbide Nuclear Division.

Description of Filling Facility

A flowsheet of the filling system is shown in Fig. 3, and Fig. 4 is an isometric drawing giving the physical relationship of components. A complete list of drawings is given in Appendix A.

The filling system comprised an electrically heated salt reservoir, and assembly of up to 15 heat storage tubes located in a vacuum chamber, a transfer (fill) line connecting the salt reservoir to a manifold located at the bottom of the heat storage tubes, argon-cooled freeze valves located at the bottom of the individual heat storage tubes and on the single overflow line, and an argon cooling duct installed in the center of each heat storage tube to remove heat after the tubes had been filled. An electric heater was provided in the center of the tube

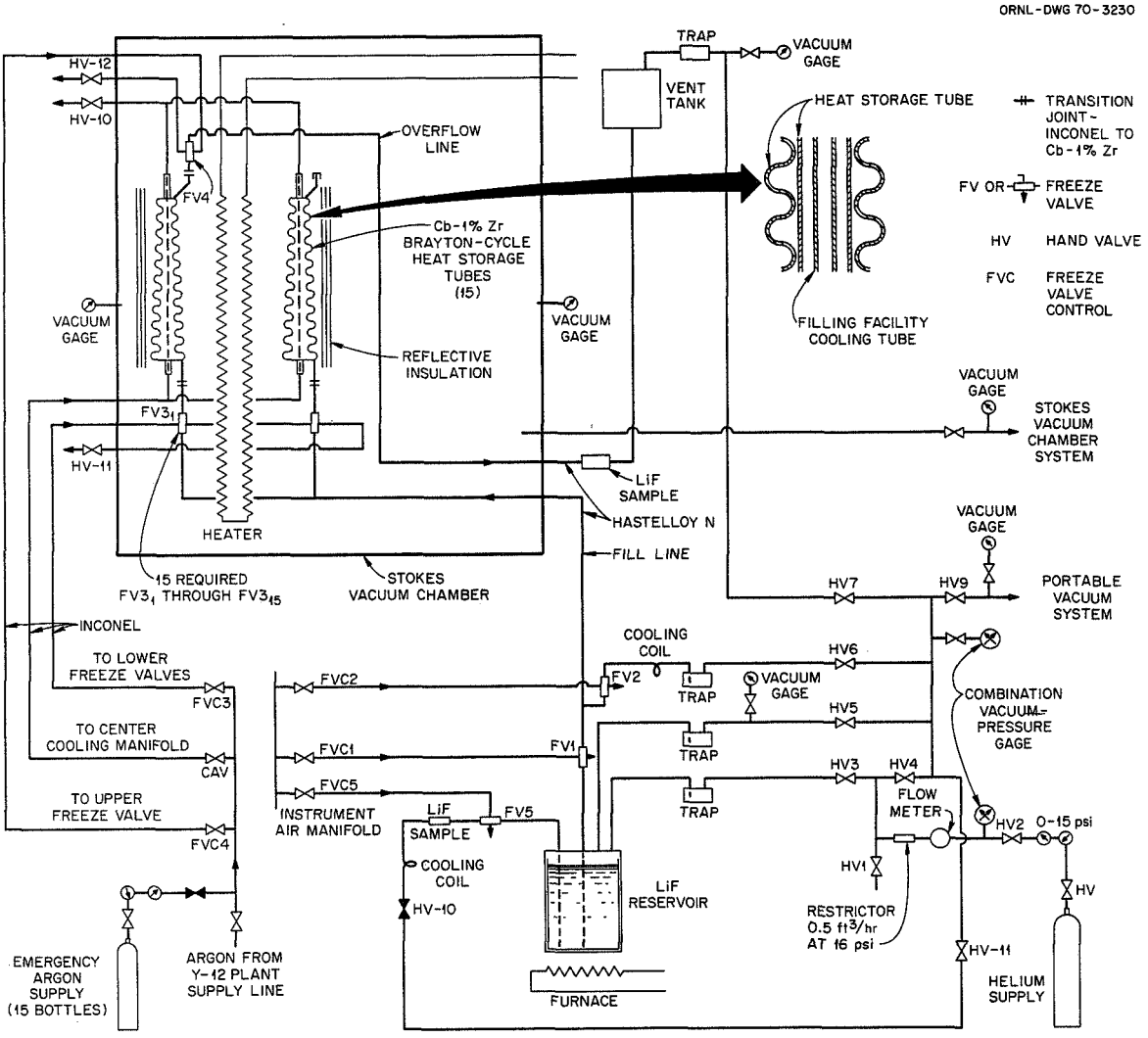

Fig. 3. Flowsheet of Facility for Filling Brayton-Cycle Heat Storage Tubes.

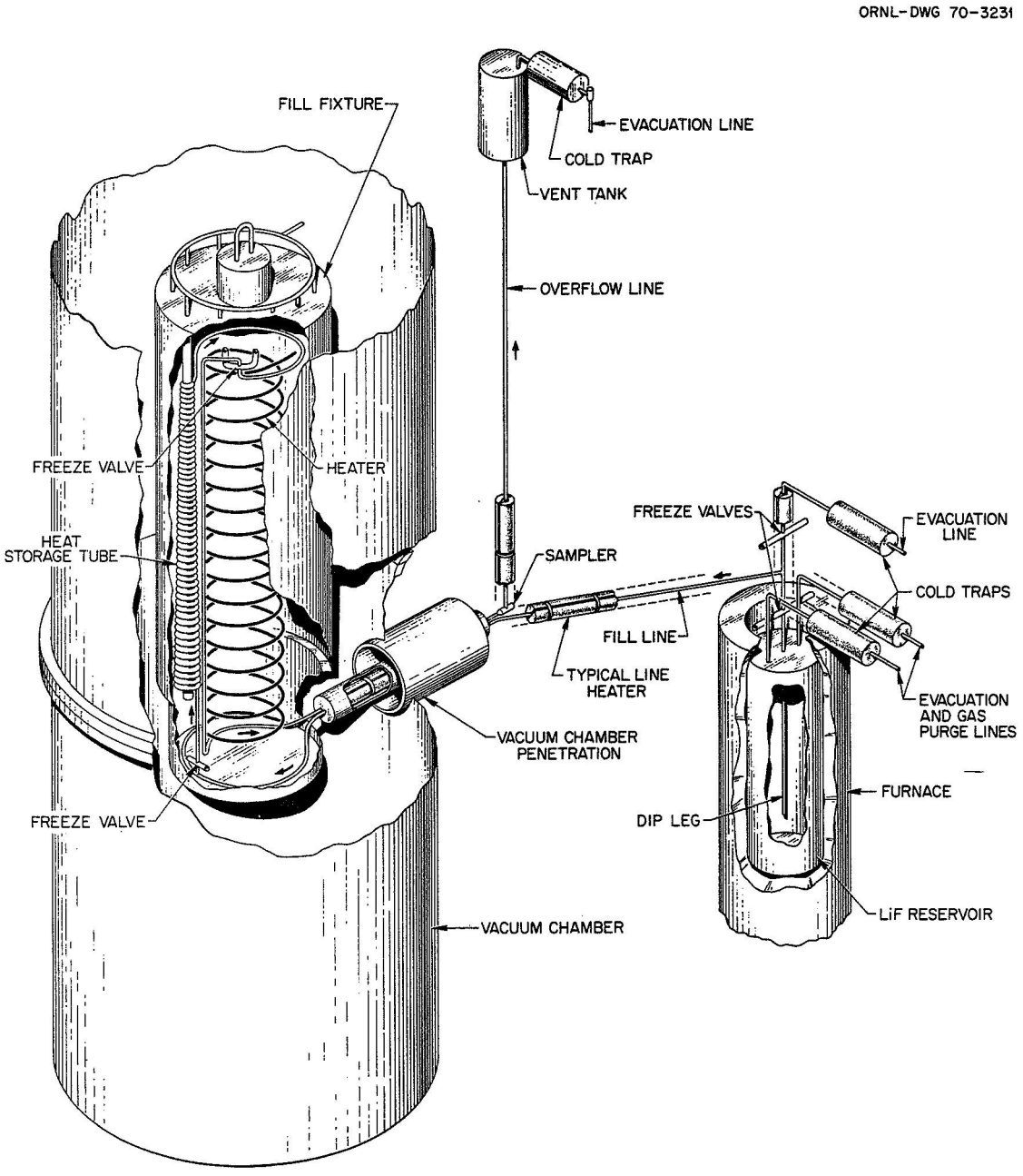

Fig. 4. Isometric Drawing of Filling Facility.

assembly. Air-cooled freeze valves were installed in the fill line from the salt reservoir to prevent accidental filling of the heat storage tubes. Vapor traps were installed on the salt reservoir vacuum lines to prevent salt vapor from contaminating the vacuum pump. A helium bottle and associated piping provided for pressurizing the salt reservoir.

The filling operation was accomplished by applying gas pressure to molten lithium fluoride in the salt reservoir. A dip leg in the tank allowed the lithium fluoride to flow upward into the heat storage tubes. When indication of complete filling was obtained, freeze plugs were created at the bottom of each of the tubes before the tube assembly was cooled.

Design Calculations

Piping and Pressure Vessels

Calculations were made and reviewed by the ORNL Pressure Vessel and Piping Review Committee in accordance with the ORNL Standard Practice Procedures. Piping flexibility calculations were made by using the piping flexibility analysis program developed by Mare Island Naval Shipyard (MEL-21P) on the IBM 7090 computer to assure conformance with the ASA Piping Code B-31.1, Code for Pressure Piping. Pressure vessels were reviewed for conformance to Section VIII of the ASME Boiler and Pressure Vessel Code.

The piping flexibility calculations disclosed that the resultant stresses exceeded the code allowable stress; however, data in ASME Paper No. 64-MET-2 by A. E. Carden indicated that the piping would have a fatigue life greater than that required. Approval for the use of the material (see App. B) was given on the basis of the short duration of use and the small number of thermal cycles required.

The salt reservoir operating temperature was beyond the maximum allowable for Hastelloy N and Inconel 600 given in Section VIII of the ASME Boiler and Pressure Vessel Code. Allowable stresses were determined for Inconel 600 at 1800°F by using the code basis for establishing stress

values and data contained in Inco Technical Bulletin T-7. The 2-in.-thick heads in the reservoir were specified on the basis of this allowable stress. Data reported for Hastelloy N indicated that the calculated stress in the 3/8-in. shell would be satisfactory at the design conditions for the lifetime of the test (see App. B).

Heat Transfer

Heat transfer calculations were made by using necessary simplifying assumptions to help verify that (1) a 20-kw radiant heater would be sufficient to bring the heat storage tube assembly to 1750°F in an acceptably short time, (2) a freeze plug would form at the 0.005-in. annulus between the root of the bellows convolution and the center tube, and (3) temperature variations across a bellows convolution or along any heat storage tube would be within acceptable limits. Since the assembly was installed in a vacuum, heat transfer was limited to radiation and conduction. Reflective insulation was installed in a manner to minimize conduction through the layers. The effect of conduction along penetrations through the reflective insulation was not included in heat loss calculations. Past applications of similar heaters and reflective insulation indicated that end losses through penetrations in the reflective insulation were insignificant with relation to the total heat transferred. However, these penetrations can produce local cold spots, so consideration was given to this problem in the design.

In calculations of radiant heat transfer through reflective insulation the expression

$$Q_n = Q/(1 + n) \qquad (1)$$

gives acceptably accurate results. In this expression n is the number of reflective layers, Q is the heat transfer that would result with no reflective insulation, and Q_n is the heat transfer experienced with n reflective layers. According to Kern,[2] Eq. (1) applied only to infinite and parallel planes separated by additional planes that are opaque to direct radiation, extremely thin, and all have the same emissivities. The system under discussion was previously described as a centrally

mounted tantalum heater element surrounded by the tube array and a columbium–1% zirconium shell on which were mounted reflective layers of stainless steel. This cylindrical geometry exposed to a stainless steel vacuum chamber wall as a heat sink only approximates these limits; however, the relationship had been used in the past for similar geometries and materials with good agreement between calculated and experimental heat losses.

From the Stefan-Boltzman equation and the above relationship, losses were calculated to be 9.5 kw. An emissivity factor of

$$\frac{1}{\frac{1}{E_1} + \frac{A_1}{A_2}\left(\frac{1}{E_2} - 1\right)} \qquad (2)$$

was used, where

E_1 = source emissivity,

E_2 = receiver emissivity,

A_1 = source heat transfer area,

A_2 = receiver heat transfer area.

This factor applies to infinite concentric cylinders or concentric spheres. Since the area ratio is small, the accuracy of calculation depends more on source emissivity than sink emissivity. The source emissivity varies with roughness and surface condition and is uncertain. The tubes intercept radiation from the heater to the reflective insulation and thus add complication and uncertainty to the problem. Measurements of electrical power to the heater during the filling process indicated the actual losses to be about 10 kw, which is very satisfactory if the many uncertainties in the system are considered.

The 20-kw design rating of the heater gave a heatup time of 3 hr. This time element was considered to be unimportant, since the heatup time of the lithium fluoride in the salt reservoir was limiting.

It was necessary to determine that the lithium fluoride would freeze rapidly at the 0.005-in. annulus between the root of the bellows convolution and the center tube and thus prevent flow between convolutions. Although heat transfer from the 1 1/4-in.-diam center tube to the 3/4-in.-

diam argon cooling tube would be by radiation only, the amount of heat transfer required to freeze a 0.005-in.-thick sleeve of lithium fluoride was small, and it was postulated that freezing would occur rapidly.

Cooling calculations were made for both helium and argon as coolant gases. Air could not be used because of the possibility of a leak and the predictable effect of air on the hot columbium–1% zirconium alloy. Argon was chosen over helium on the basis of cost.

The foil wrapping on the central cooling tube added more uncertainty to the calculations. It was difficult to predict whether this foil would be loose enough to act as a reflective layer or tight enough to add very little resistance to heat transfer. A factor of approximately two difference in heat transfer depends on the assumption used. Therefore a test of the cooling effectiveness was made early in the program when a single stainless steel tube was filled with lithium fluoride. Cooling of this stainless steel tube was accomplished by passing argon through three 1/4-in.-OD tubes installed inside the test tube. The actual argon requirement was not in good agreement with the calculated argon requirement; however, the predicted rapid freezing of the lithium fluoride at the root of the convolutions was verified during this test. The freezing effect was again checked when a single columbium–1% zirconium tube was filled in the vacuum chamber. The cooling duct in subsequent assemblies was changed from the three 1/4-in. tubes to one 3/4-in. tube. This change was possible when the design of the heat storage tubes was changed to eliminate internal fins in the central tube.

An attempt was made to show by calculation that temperature variations along and across each tube during heatup and cooldown would not be excessive. There appeared to be little possibility of a problem across the diameter of any convolution, but variation in temperature along the length of the tube could be expected. These variations in the actual tests were determined to be ±20°F, with one tube installed in the assembly. The 15 tube assemblies gave variations of ±30°F. The main cause of these variations was the penetration of the central cooling tubes through the reflective insulation at the top and bottom of the assembly and the resulting outward conduction of heat.

Equipment Components, Fabrication, and Assembly

Heat Storage Tube Preparation

The heat storage tubes received from NASA Lewis Laboratory were complete with 0.156-in.-OD, 0.018-in.-wall fill and vent tubes attached. Upon receipt the tubes were helium leak checked by placing them in a plastic bag, evacuating the volume of the tube to be filled with salt to less than 0.10-μ pressure, and then flooding the bag with helium. Any indication of a leak after 20 min by a Consolidated helium leak detector was cause for rejection. The leak detector sensitivity was always greater than 1×10^{-10} cc/sec, as measured by a standard leak.

Some bowing was discovered when the first heat storage tubes were received at NASA Lewis Research Center, and the straightness checks indicated that the bowing had occurred during shipment. New crating techniques for shipment were employed, and the bowing was eliminated, as indicated by later checks.

The transition joints used to attach the columbium–1% zirconium fill tubes to the Hastelloy N parts of the filling system were then attached to the tubes. The design of these joints which were developed and tested by the ORNL Metals and Ceramics Division, is shown in Fig. 5. The columbium–1% zirconium and Inconel 600 assemblies were vacuum furnace brazed with Nicrobraz 200 at 1950 to 2150°F. Helium leak checking and ultrasonic testing were used to determine joint integrity.

During development of this transition joint, ten test pieces were fabricated for thermal-cycling tests to prove their adequacy for the intended service. The most severe test was of 192 hr duration at 1775°F with six thermal cycles between 1775°F and room temperature. All ten joints were helium leak checked and ultrasonically tested and found to be acceptable.

The columbium–1% zirconium fill and vent tubes (0.156 in. OD, 0.018 in. wall) were cut to proper length, and columbium–1% zirconium to Inconel transition joints were welded to the bottom end. These columbium–1% zirconium welds and a columbium–1% zirconium closure weld on the vent tubes

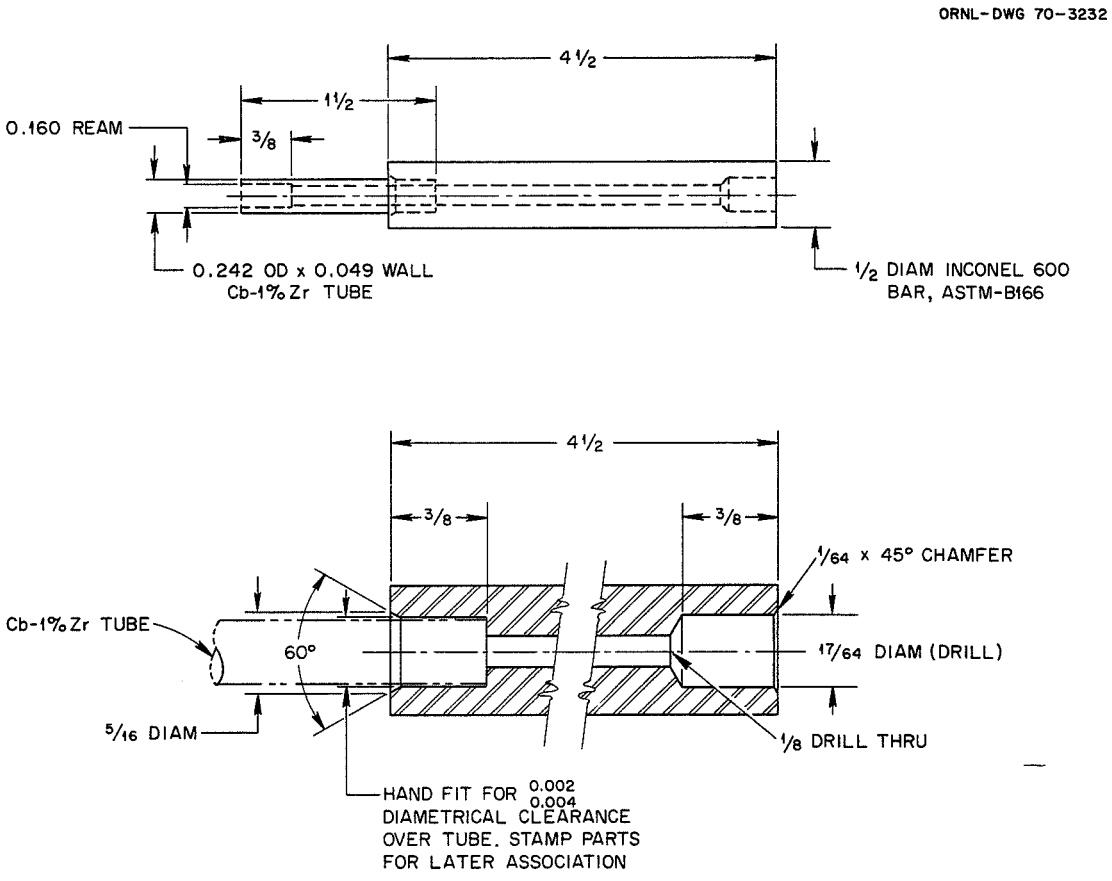

NOTE:

1. FURNACE BRAZE WITH NICRO-BRAZE-200 (7% Cr, 3.2% B, 3% Fe, 4.5% Si, 6% W, BALANCE Ni) AT 1950-2150°F IN A VACUUM OF $\sim 5 \times 10^{-5}$ torr.
2. ULTRASONICALLY CHECK TO SPECIFICATION MET-NDT-3 WITH SPECIAL STANDARD AFTER BRAZING.
3. HELIUM LEAK CHECK AFTER BRAZING.

DIMENSIONS ARE IN INCHES

Fig. 5. Transition Joint Between Columbium–1% Zirconium Fill Line and Inconel 600 Transfer Line.

at the top end were made in an argon atmosphere drybox in the ORNL Welding and Brazing Facility (see Fig. 6). The drybox and pumping system were capable of vacuums to 5×10^{-5} torr. A purging system that used high-purity argon was attached to the box. Prior to welding, a weld pass was run on a block of zirconium metal to getter any excess oxygen or mositure.

Oxygen and moisture impurity levels in the drybox were monitored with a coupon of stainless steel. A very light straw color of the stainless steel metal as a 1/8-in. weld pass was made indicated that oxygen and moisture levels were below 5 ppm. Any blue discoloration was cause to suspect contamination in the atmosphere. Practice welds on stainless steel coupons provided these visual calibrations based on measurements made with a Manufacturers Engineering & Equipment Company, Model O electrolytic oxygen analyzer and a Model W electrolytic moisture analyzer. Details of the drybox procedures are presented in Appendix C.

The sleeve welds and the plug welds were radiographed and liquid-penetrant checked in accordance with ORNL Metals and Ceramics Division Specifications NDT-4 and -5, respectively. After these welds were made and inspected the heat storage tubes were again helium leak checked and weighed, and a volumetric measurement was made by pressure decay in a known volume vented to the tube.

The assembly of the heat storage tubes into the fixture was accomplished in a controlled access room. Workers in the assembly room wore shoe scuffs and nylon gloves, and a recirculating filtered air system kept airborne material to a miniumum.

All welds were made to appropriate ORNL Metals and Ceramics Division specifications. The welds were radiographed and liquid-penetrant checked in accordance with ORNL Metals and Ceramics Division specifications NDT-4 and -5, respectively.

In addition to the normal materials handling and cleaning procedures, the specifications given in Appendix D were used. These procedures were also used for work associated with installation of equipment in the vacuum chamber.

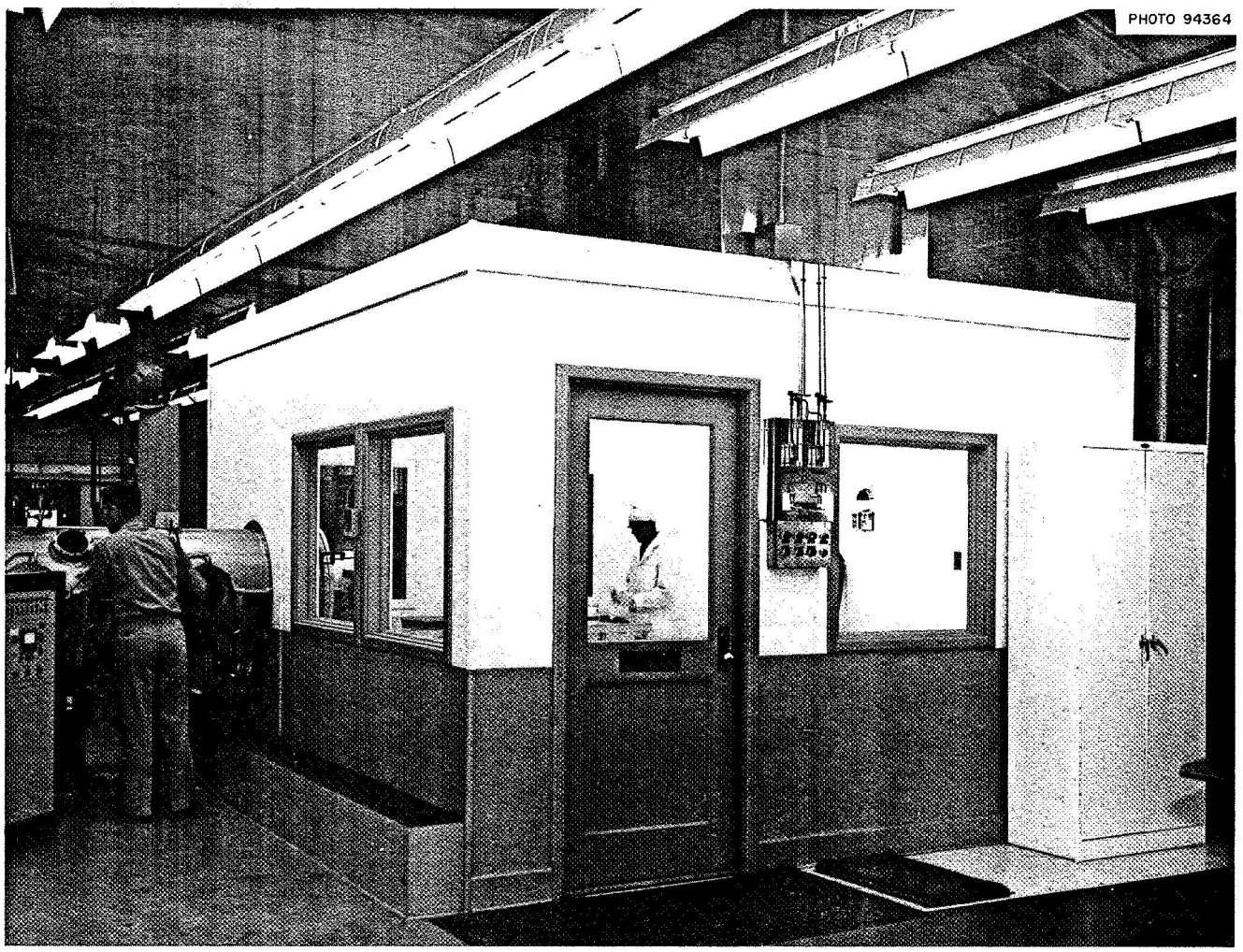

Fig. 6. Clean Room and Dry Box Welding Facility in ORNL Building 7003.

All stainless steel thermocouples and nickel-base alloys used inside the assembly fixture were wrapped with a layer of columbium–1% zirconium or tantalum foil to protect the heat storage tubes from contamination.

Helium leak checks were made at appropriate stages of the assembly sequence. All leak detection was accomplished by using a mass spectrometer-type leak detector that was sensitive to 1×10^{-10} cc/sec leakage, as measured by a standard leak, and any detectable leakage was cause for reworking.

Heat Storage Tube Assembly Fixture

The assembly fixture for batch filling the heat storage tubes was designed to accept 15 tubes. The lower supports and assembled tubes are shown in Fig. 7. The 15 heat storage tubes were positioned vertically on the support plate and spaced at equal intervals on a 17 3/32-in.-diam circle. The support plate was fabricated from 0.050-in.-thick columbium–1% zirconium material. Studs to position the tubes projected through the top support plate. Specially designed clips were used at the top of the assembly to center each tube on its argon cooling duct, which was installed vertically through the center portion of the tube.

As mentioned above, a 0.156-in.-diam 0.018-in.-wall columbium–1% zirconium tube was welded to the bottom and top convolution of each of the heat storage tubes. The 0.156-in. tubes attached to the bottom convolutions were used for filling the heat storage tubes. In each 15-tube assembly, one of the 0.156-in. tubes attached to a top convolution was used as an overflow tube to collect a lithium fluoride sample. Thermocouples attached to the overflow line were used to indicate that the salt had been raised to the required level. The 0.156-in. tubes attached to the top of the other 14 heat storage tubes were seal-welded approximately 4 in. above the top convolution, and thermocouples were attached to each tube at the seal-welded tip.

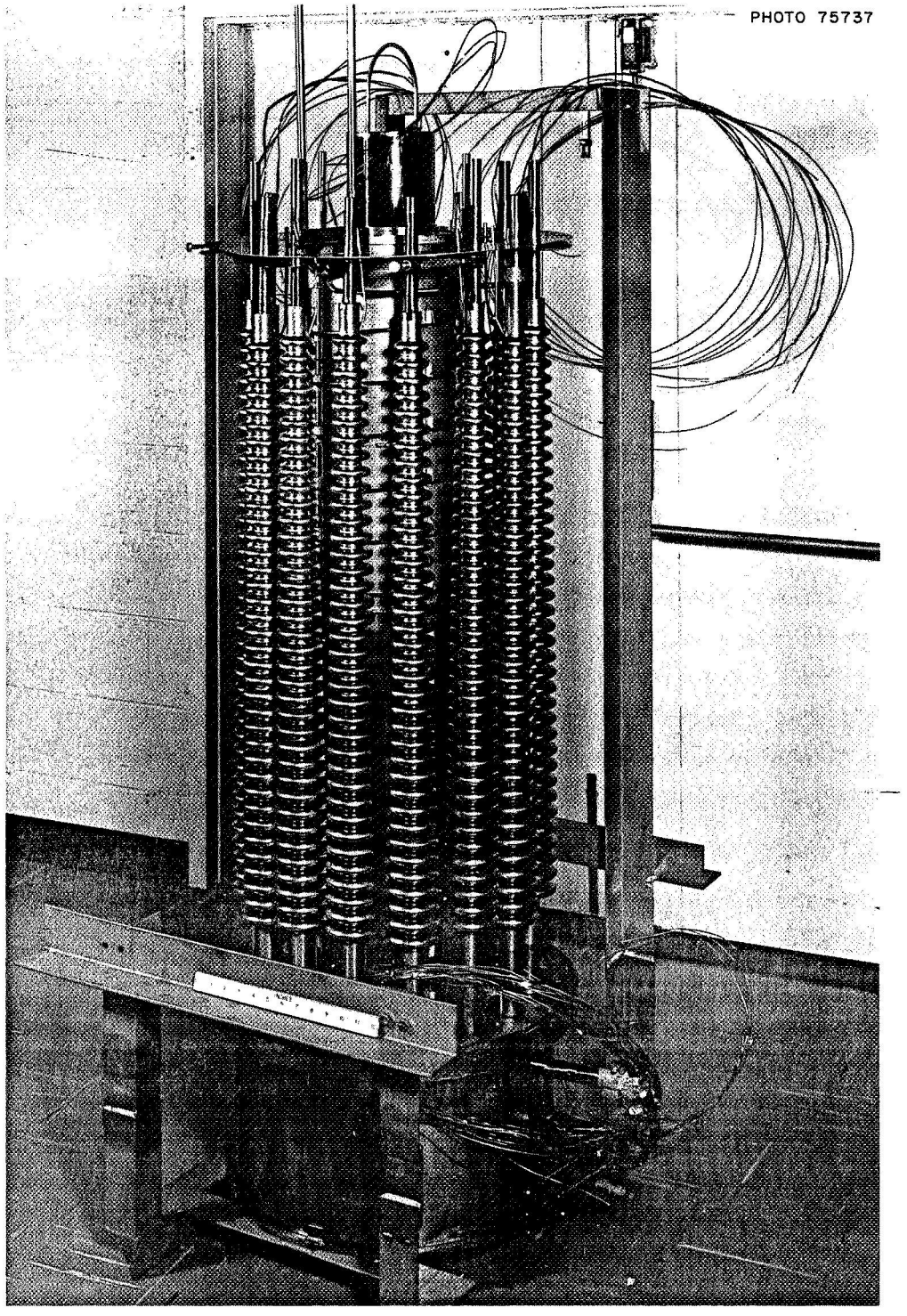

Fig. 7. Heat Storage Tubes in Assembly Fixture.

The fill tubes at the bottom of each of the heat storage tubes were attached to a 3/8-in.-OD 0.035-in.-wall Hastelloy N ring manifold (see Fig. 8), which was located below the above-mentioned support structure. Salt from the reservoir entered the ring manifold through a 1/4-in.-OD 0.065-in.-wall Hastelloy N tube.

Approximately 2 1/2 in. above the ring manifold a freeze-valve line was installed on each of the vertical fill tubes feeding the heat storage tubes. The freeze valve consisted of a single 1/2-in.-OD x 0.065-in. Hastelloy N tube formed to the same circle diameter as the filling manifold (see Fig. 8). Fifteen holes were drilled through both walls of this freeze-valve line, and the filling lines projected through it. Seals in the form of fillet welds were made to both walls of the freeze-valve line. Attachments of gas inlet and outlet lines were made at one side of the freeze-valve ring. In the latter stages of the fill operation, high-velocity argon was admitted to this freeze-valve line, and a freeze plug was formed where each of the fill lines passed through the freeze-valve line. Thus, a single argon stream served to cool all the freeze valves in the inlet salt lines to the heat storage tubes.

The center cooling ducts were welded at the top and bottom of the assembly to a 1-in. sched-40 Inconel pipe, which was formed in a 17 5/64-in.-diam circle to match the spacing of the heat storage tubes. The inlet (or bottom) manifold was connected to an argon supply and was the distribution header for the cooling argon to the 15 heat storage tubes. The similar manifold at the top of the assembly (see Fig. 9) acted as a collector for the hot gas at the outlet.

The central radiant heater projected from the bottom of the salt inlet ring manifold to the top of the heat storage tubes (see Fig. 10). This 20-kw heater (Fig. 11) was fabricated by spirally winding 3/16-in.-diam tantalum rod on a 3 1/4-in. pitch to a diameter of 10 in. This coil was attached by alumina insulators, rated for 1950°C service, to a 58.5-in.-high 9-in.-diam cylinder of 0.050-in.-thick columbium-1% zirconium. Electrical leads were attached to the tantalum heater coil at three points (two parallel heater circuits) by 1/2-in.-diam tantalum

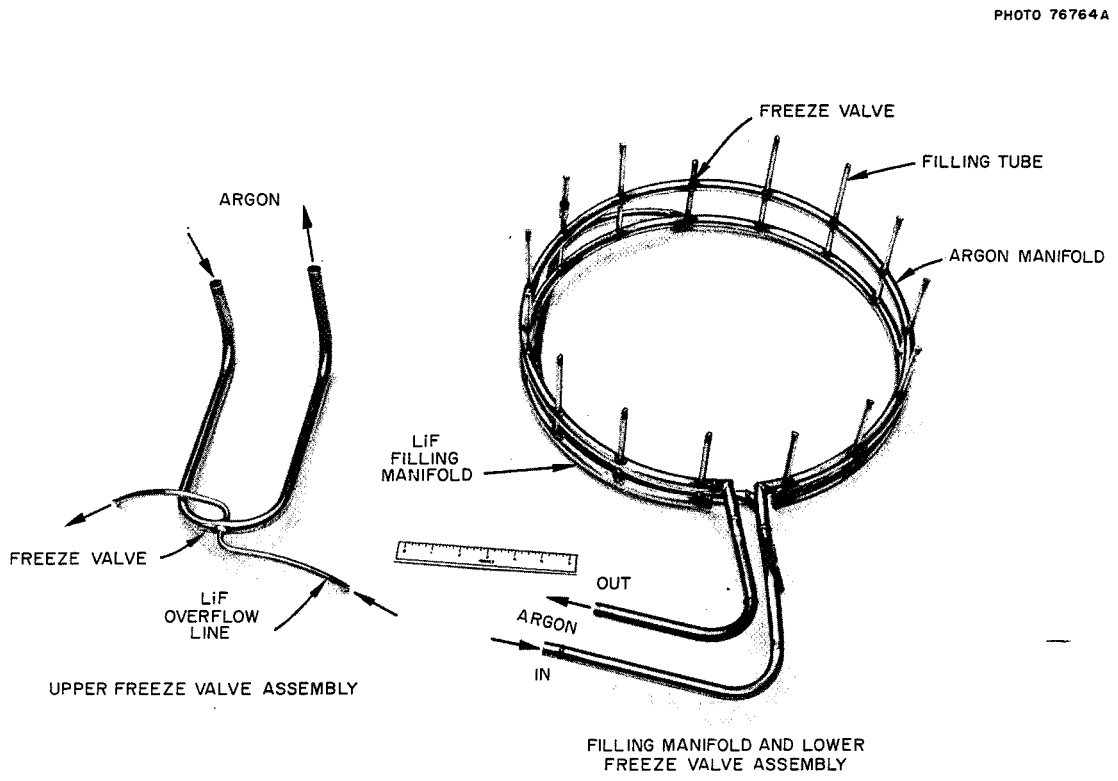

Fig. 8. Upper Freeze Valve and Lower Freeze-Valve Manifold.

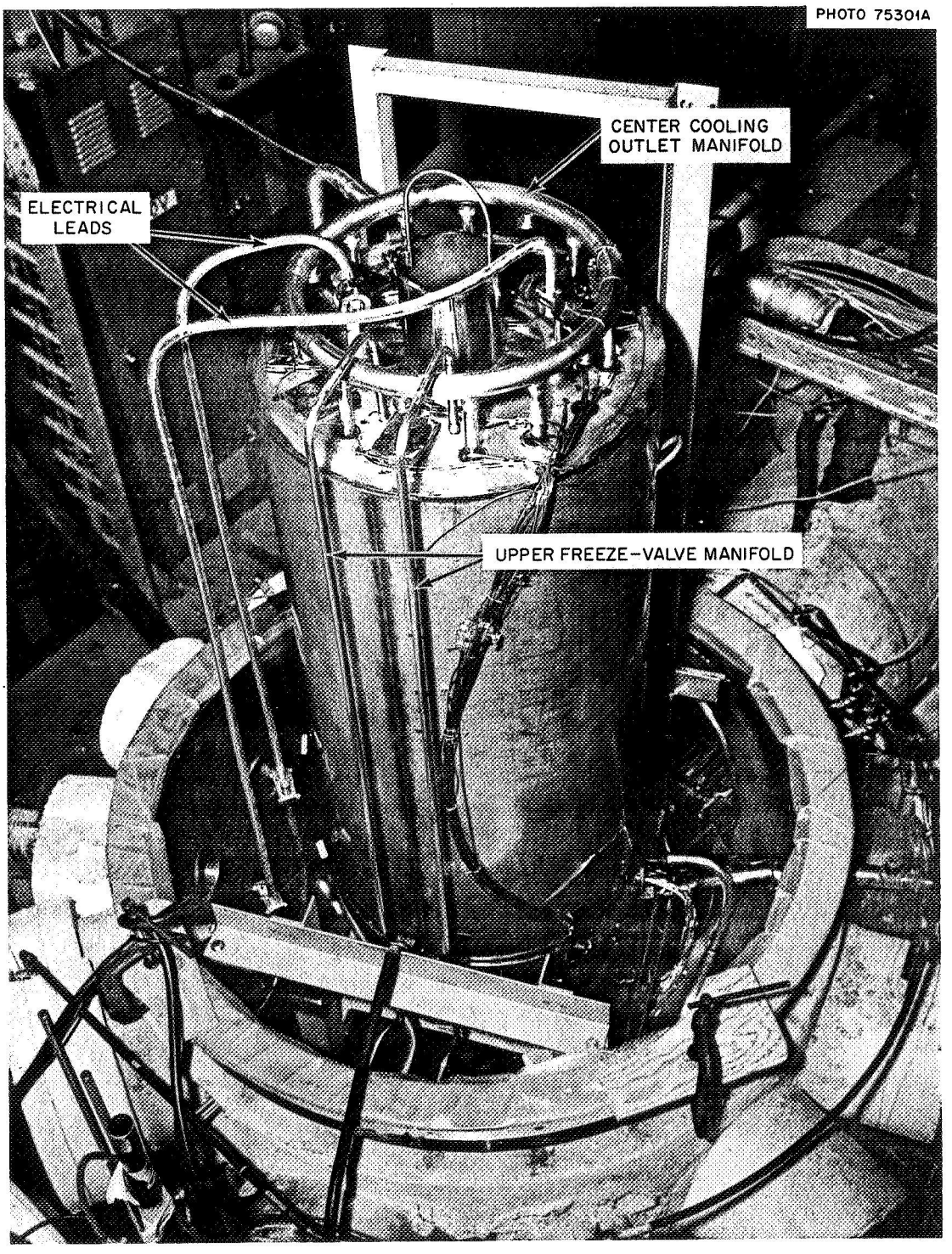

Fig. 9. Heat Storage Tube Assembly Installed in Vacuum Chamber Bowl.

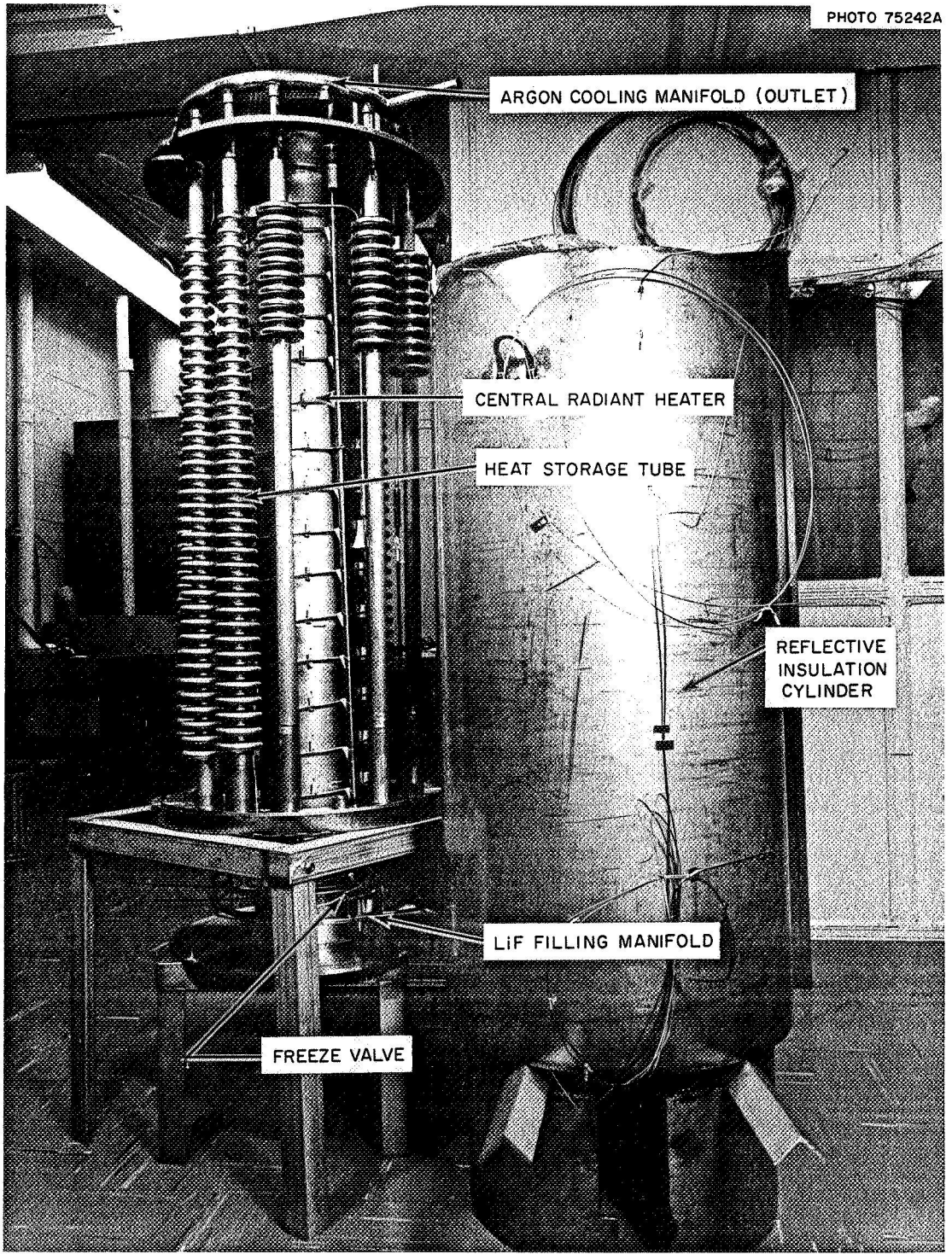

Fig. 10. Heat Storage Tube Assembly Showing Central Radiant Heater.

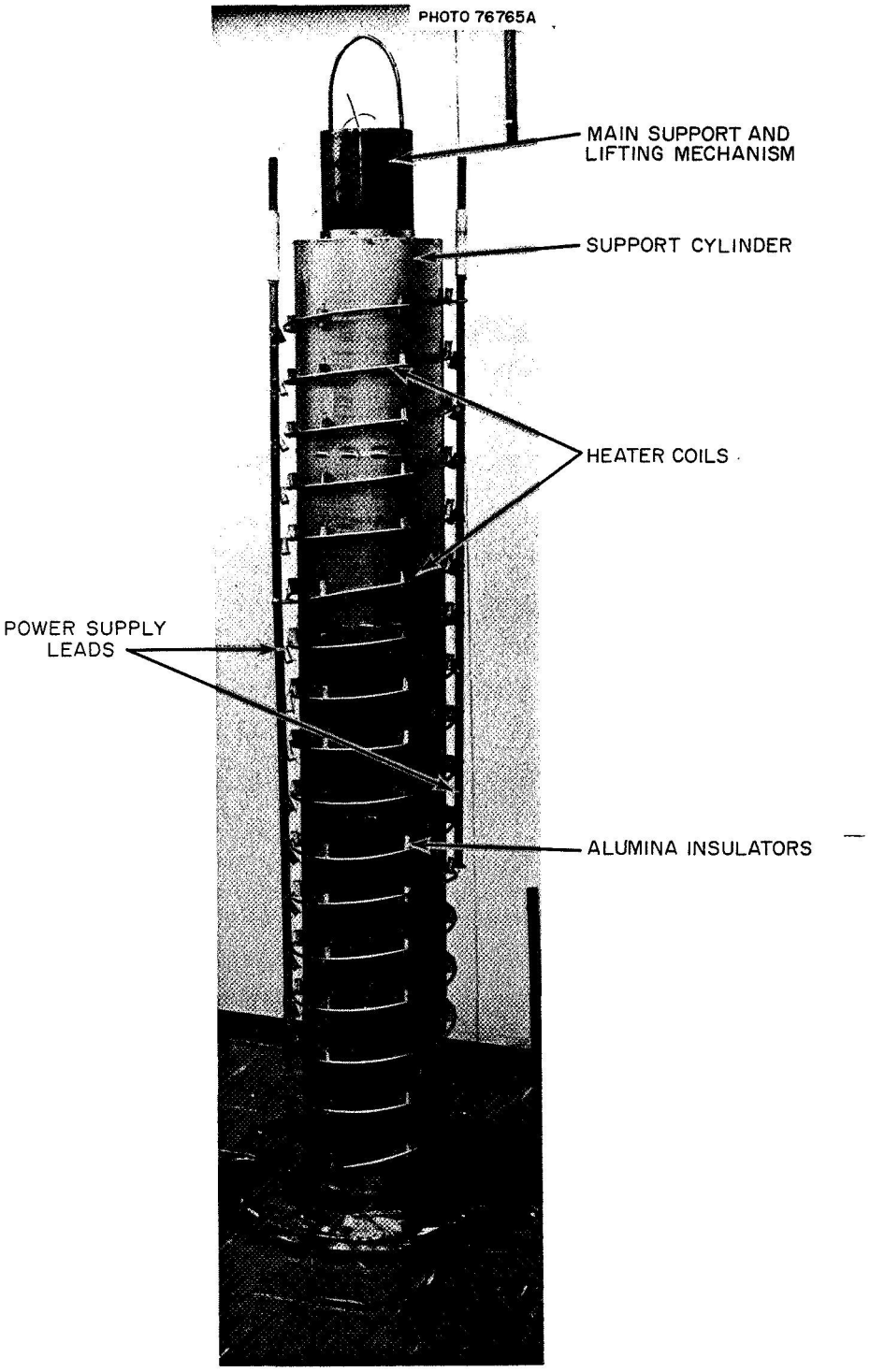

Fig. 11. Central Radiant Heater Assembly.

rods. These rods were installed vertically and extended above the top of the assembly, where copper bus bars were attached in the final stages of installation. Reflective insulation was installed around the cylindrical assembly. This heater was operated to a maximum of 11 kw at 26 v and 430 amp.

Magnesium oxide-insulated, type 304 stainless steel-sheathed, 1/16-in.-OD thermocouples were installed on the assembly as shown in Fig. 12. These thermocouples were purchased to ORNL specification I.S. 124-1. All the thermocouples and nickel-base alloys used inside the assembly fixture were wrapped with a layer of columbium—1% zirconium alloy or tantalum foil to protect the heat storage tubes from contamination.

The outer thermal insulation shells (see Fig. 12) were formed from layers of columbium—1% zirconium alloy and stainless steel. Two cylindrical assemblies were formed. The upper cylinder, which surrounded the heat storage tubes, was 23 in. in diameter and 10 13/16 in. high. Both cylinders were formed by placing six layers of 0.020-in.-thick stainless steel and two layers of 0.020-in.-thick columbium—1% zirconium sheet inside a 1/16-in.-thick type 304 stainless steel sheet. The layers of columbium—1% zirconium and stainless steel sheets were separated by 0.062-in.-diam wire spacers located approximately 4 in. apart.

The lower cylinder rested on a base plate of Hastelloy N material 3/8 in. thick and 21 in. in diameter. It was the main support for the entire heat storage tube assembly, including the central heater. A 10-in.-high 30° segment was removed from this lower cylinder. The lithium fluoride fill line, overflow line, lower freeze-valve inlet and outlet lines, the center cooling supply line, and some of the thermocouples passed through this opening. Specially fabricated thermal insulation patches of the laminated design closed these penetrations (see Fig. 13). Similarly, laminated disks of stainless steel and columbium—1% zirconium sheet were fabricated to form the top and bottom of the cylinder assembly. Holes were punched in the top for the center cooling ducts, the top freeze-valve inlet and outlet line, heater leads, and most of the thermocouples. Suitable laminated layers of reflective insulation were used to close these penetrations.

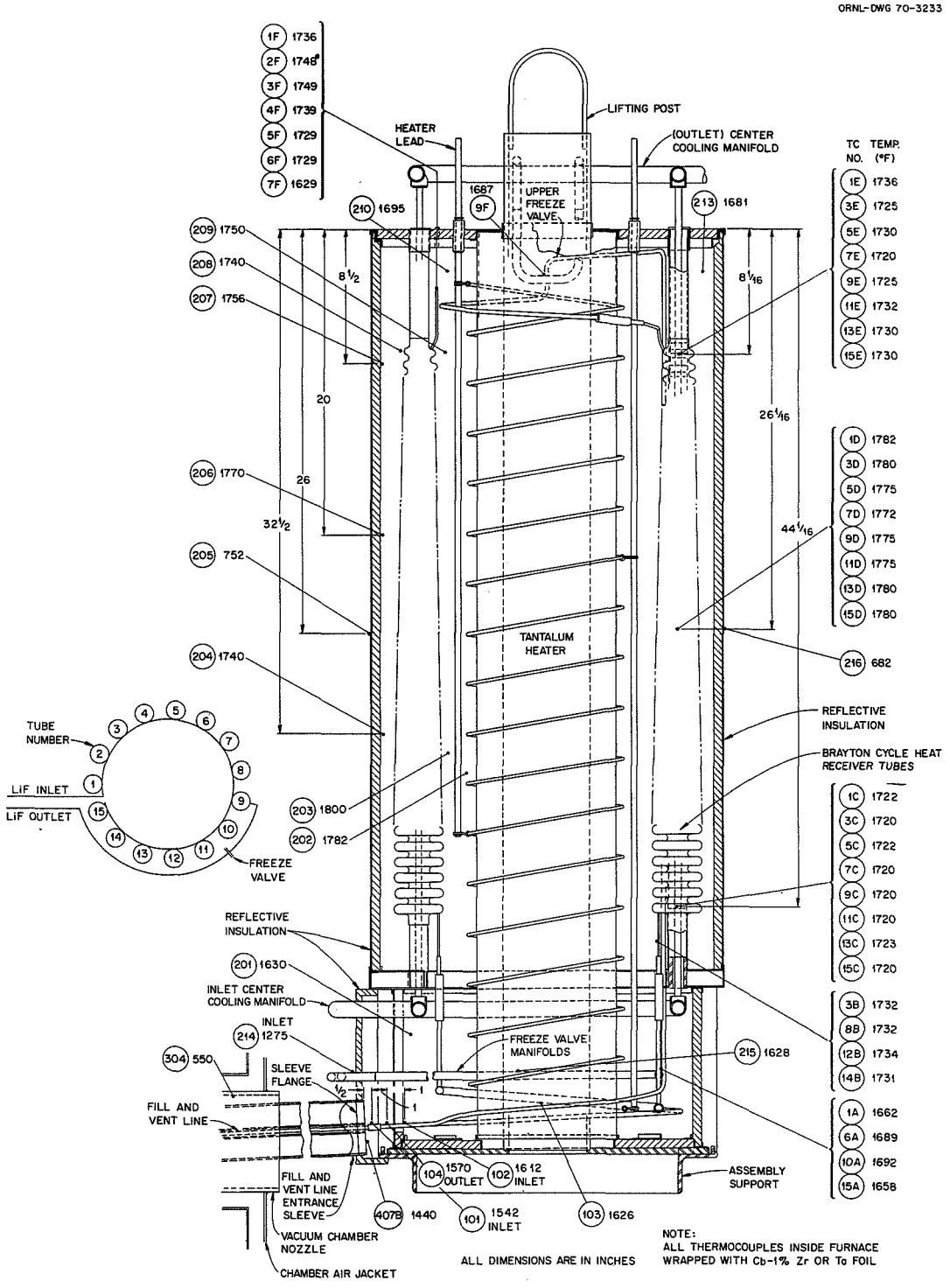

Fig. 12. Thermocouple Locations and Temperatures at Time of Tube Filling.

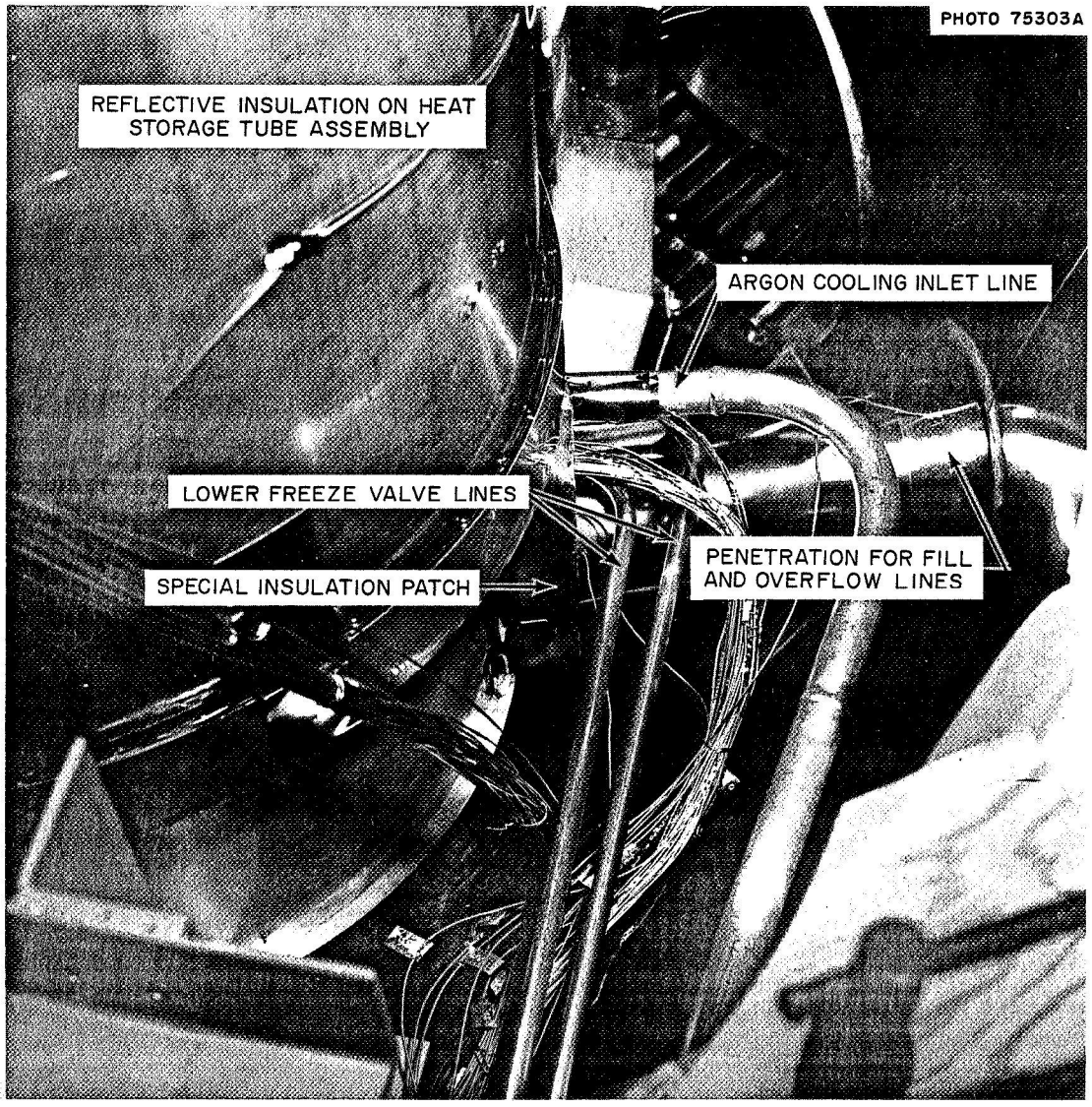

Fig. 13. View of Lower Portion of Heat Storage Tube Assembly Installed in Vacuum Chamber.

Vacuum Chamber

The assembled fixture was placed inside the vacuum chamber, which was composed of two sections: a fixed bowl 40 in. deep and a removable bell jar 90 in. high. When assembled, the pieces provided a vertical tank with an inner space 130 in. high and 49 in. in diameter. Two concentric Buna O-rings were installed in a flange between the two portions of the vacuum chamber, and the space between the two rings was continuously evacuated. The bowl portion was equipped with eight 6-in.-diam nozzles, two 12-in.-diam nozzles, and one 18-in.-diam elbow leading to the vacuum pumps. Overall views of the chamber are shown in Figs. 14 and 15. A schematic diagram of the vacuum chamber and accessories is shown in Fig. 16. The chamber was available from a previous test program.

The chamber was evacuated initially to 1×10^{-2} torr with a 40-cfm mechanical roughing pump. Two oil diffusion pumps (4 and 10 in., with capacities of 280 and 4200 liters/sec, respectively) were connected in series upstream of the roughing pump. This pumping system was designed to reduce the chamber to an ultimate pressure of 1×10^{-10} torr (when clean and empty). A 12-in. valve was installed between the 10-in. diffusion pump and the evacuation elbow on the vacuum chamber.

A cryogenic trap consisting of an 11-in.-diam 18-in.-long tank filled with liquid nitrogen was suspended in the vertical portion of the evacuation elbow above the 12-in. valve to trap any oil backstreaming from a water-cooled baffle above the 10-in. diffusion pump. As an added precaution, packets filled with a molecular sieve material were placed on the horizontal portion of the evacuation elbow.

Entrance and exit to the vacuum chamber by the fill and overflow lines presented a particular problem, since it was necessary to transfer the lithium fluoride at a temperature of 1750°F. A method of preheating the line through this penetration and an appropriate heat barrier to protect the vacuum chamber wall were required. The design of this penetration is shown in Fig. 17.

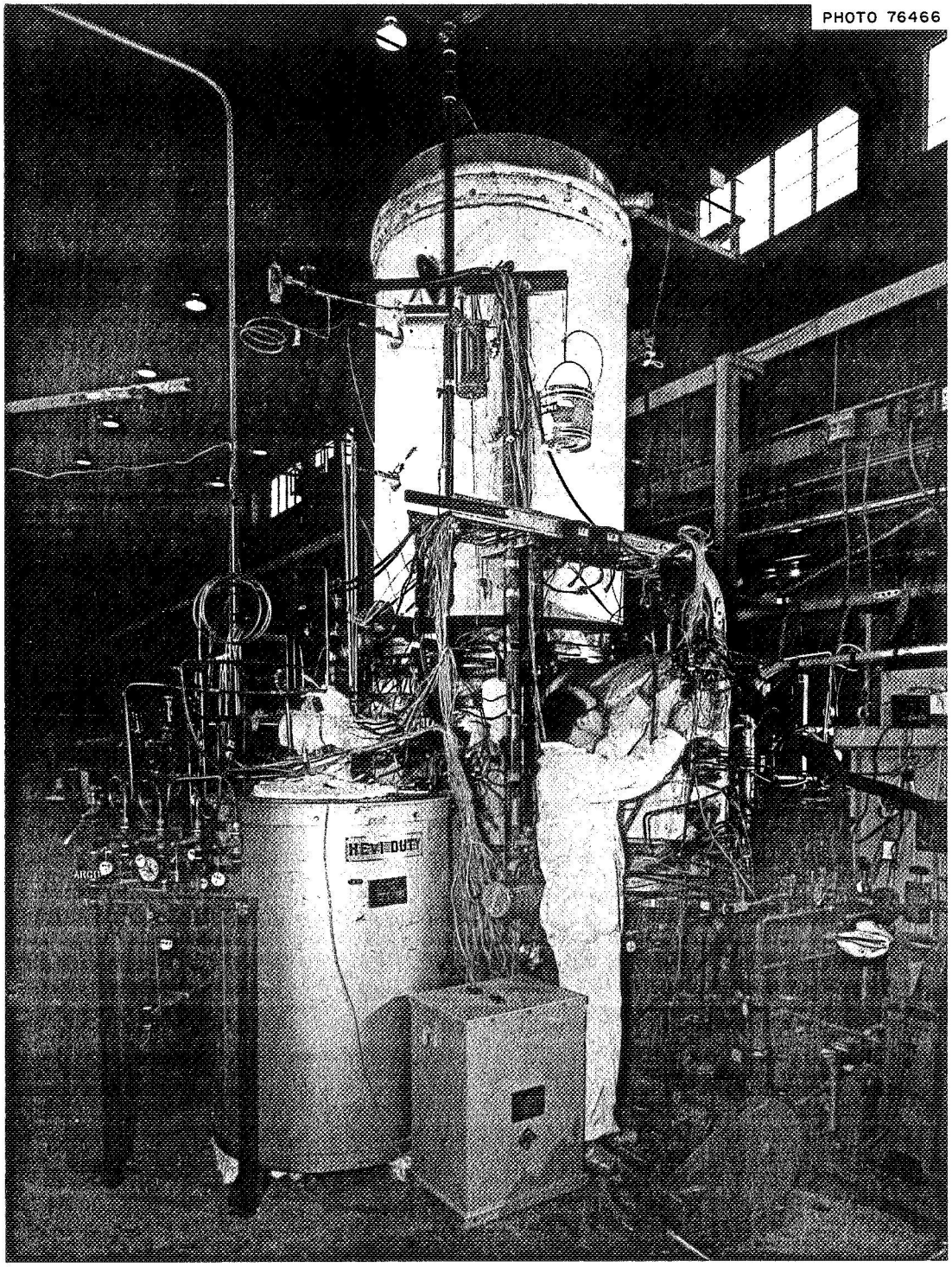

Fig. 14. Vacuum Chamber, Auxiliary Equipment, and Furnace for Heating Lithium Fluoride.

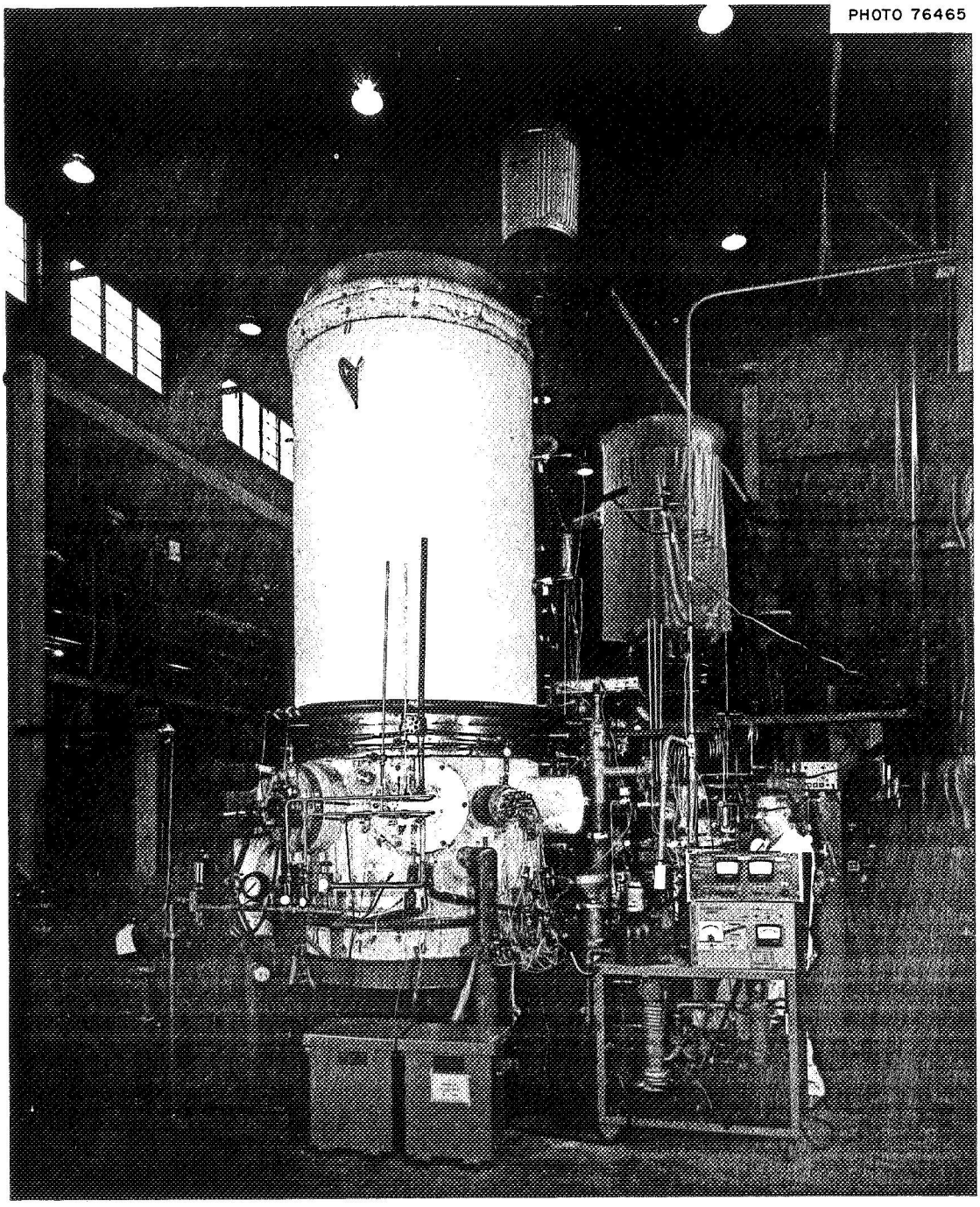

Fig. 15. Vacuum Chamber and Auxiliary Diffusion Pump Wagon for Salt Reservoir.

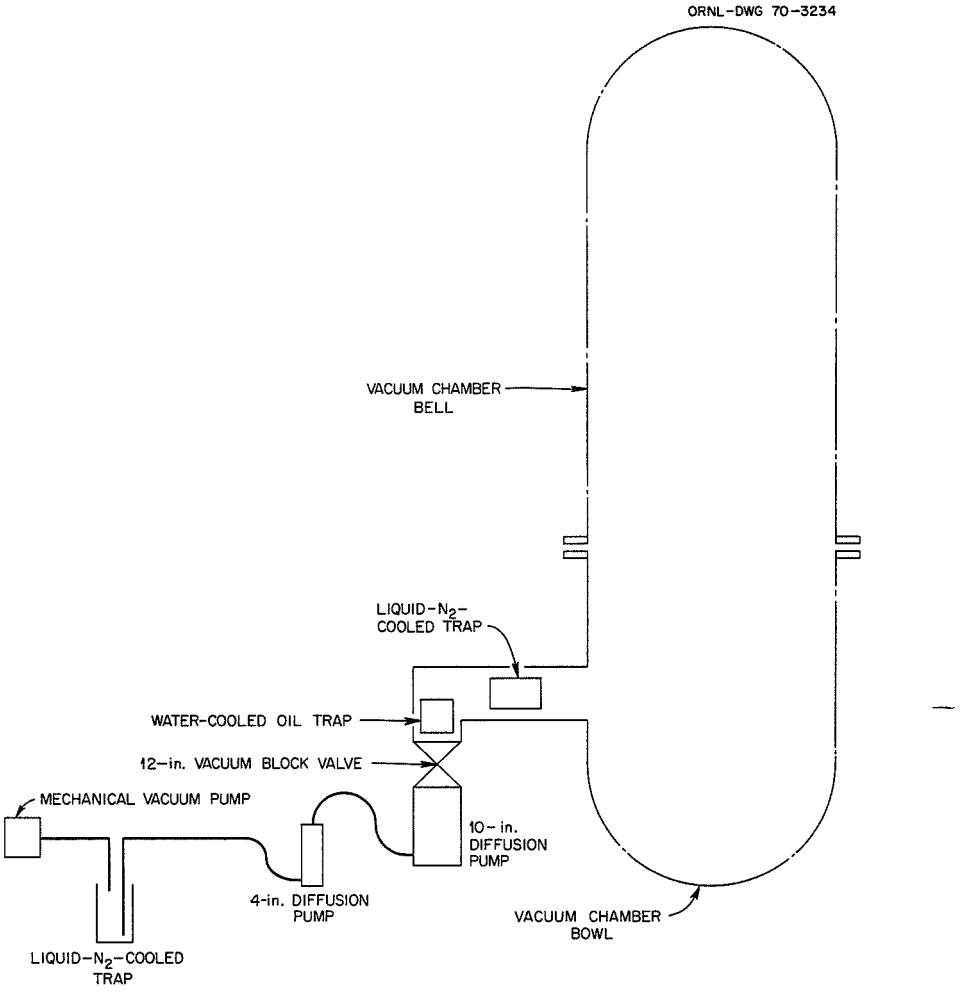

Fig. 16. Schematic Diagram of Vacuum Chamber and Evacuation System.

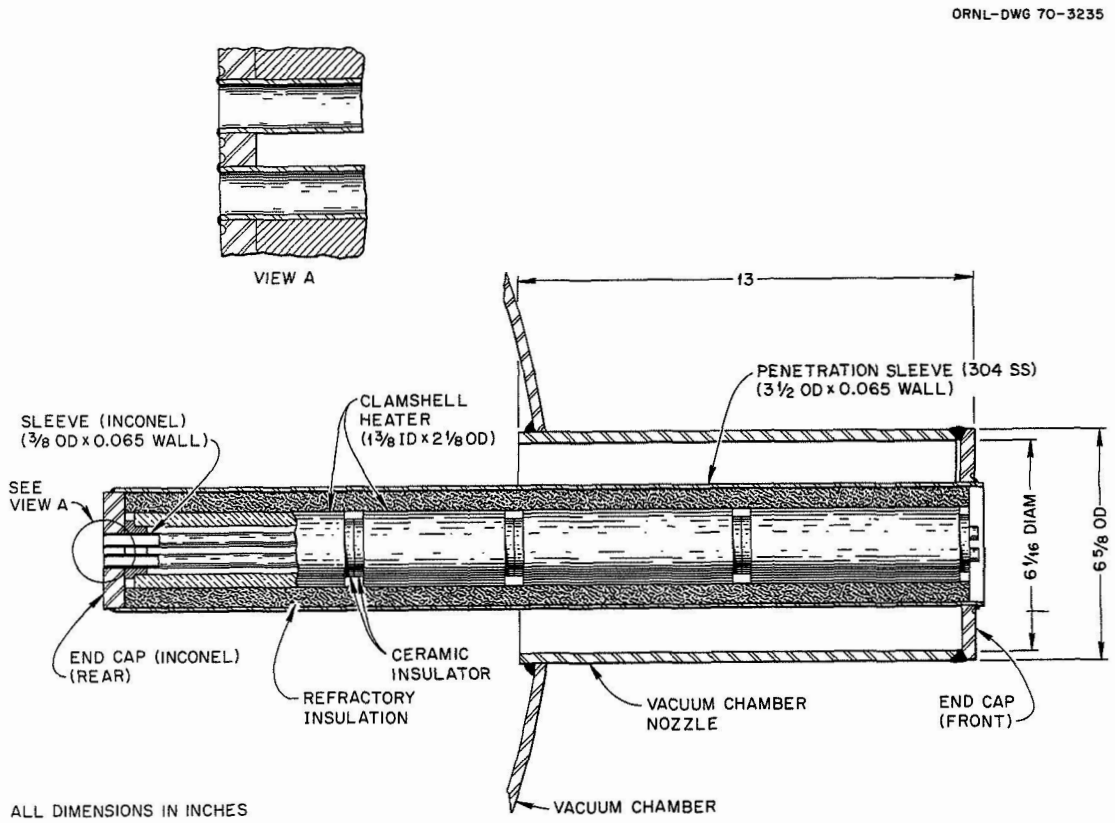

Fig. 17. Fill and Vent Line Vacuum Chamber Penetration.

Clamshell-type resistance heaters with the Nichrome-wire heating element embedded in a ceramic support material were installed around the parallel Hastelloy N fill and overflow lines. A 3 7/16-in.-diam 0.065-in.-wall container surrounded the clamshell-type heaters. A 3 23/64-in.-diam 5/8-in.-thick plate was used to close one end of the container. Johns-Mansville Kaowool insulation 1 in. thick surrounding the clamshell heaters provided a heat barrier to the barrel of the container. Nickel lead wires brought to the outside surface of the Kaowool insulation provided the voltage connection to the heater.

To eliminate cold spots at the juncture between the chamber penetration and the heat storage tube assembly furnace, it was necessary to extend the back side of this penetration to a point inside the tube assembly furnace. The outside edge of the penetration was welded to a plate, which was in turn welded to a 6-in.-diam vacuum chamber projection. Hastelloy N tubes 3/8 in. in diameter with a 0.030-in. wall were placed around the fill and overflow lines to form sleeves. One end of each sleeve was welded to the 5/8-in.-thick Inconel 600 plate that projected into the furnace. The other chamber seal was made on the outside where the 3/8-in. sleeves were welded to the fill and overflow tubes. The long heat conducting path provided by this design gave low temperatures at the vacuum chamber wall.

Two 400-amp Varian Company feed-through connectors were used for the power leads to the heating circuit inside the vacuum chamber. The 72 thermocouples for measuring temperatures inside the furnace entered through standard Teflon-insulated Conax fittings. Two nude ion gages were installed through the chamber walls to measure pressures in the 1×10^{-8} torr range. Pressures in the micron range were measured with standard thermocouple gages.

Salt Reservoir

The salt reservoir (Fig. 18) was fabricated from Hastelloy N and Inconel plate. The side walls were fabricated from 3/8-in.-thick Hastelloy N material, and the top and bottom were fabricated from 1 1/2-in.-thick Inconel plate. A 23-kw 230-v Nichrome-wire resistance-heated tube furnace was provided for heating the salt reservoir.

A 1/4-in.-diam 0.035-in.-wall Hastelloy N dip tube was installed through the top head and extended to a point 1/4 in. from the bottom of the tank. A commercial 200-ft^3 cylinder filled with high-purity helium was used to apply an overpressure to force salt upward through the dip tube. When the overpressure was applied to the top of the lithium fluoride, the salt was forced out of the tank through the transfer line and the inlet salt manifold into the heat storage tubes. Two 3/8-in.-diam 0.065-in.-wall Hastelloy N tubes also penetrated the top of the fill tank and were used as evacuation and pressure lines. Inconel 600-sheathed magnesium oxide-insulated level probes were provided. These level probes had been successfully used with other molten fluoride salts at lower (1200°F) temperatures; however, they did not operate satisfactorily during the first filling operation and were later eliminated.

Freeze valves were placed in the transfer line above the salt tank. One was located 6 in. above the tank and was used to create a frozen plug in the transfer line at the tank exit. There was a second freeze valve in a branch line from the transfer line approximately 18 in. above the tank. This branch line was one of two used to evacuate the heat storage tubes. The frozen plug in this line was established after the plug in the freeze valve just above the reservoir had been thawed and salt had been forced up high enough to enter the vacuum line. This procedure prevented the entrance of salt into the vacuum system during the subsequent filling operation. A third freeze valve was placed in another dip-leg line to use for salt sampling prior to the actual filling of the tubes.

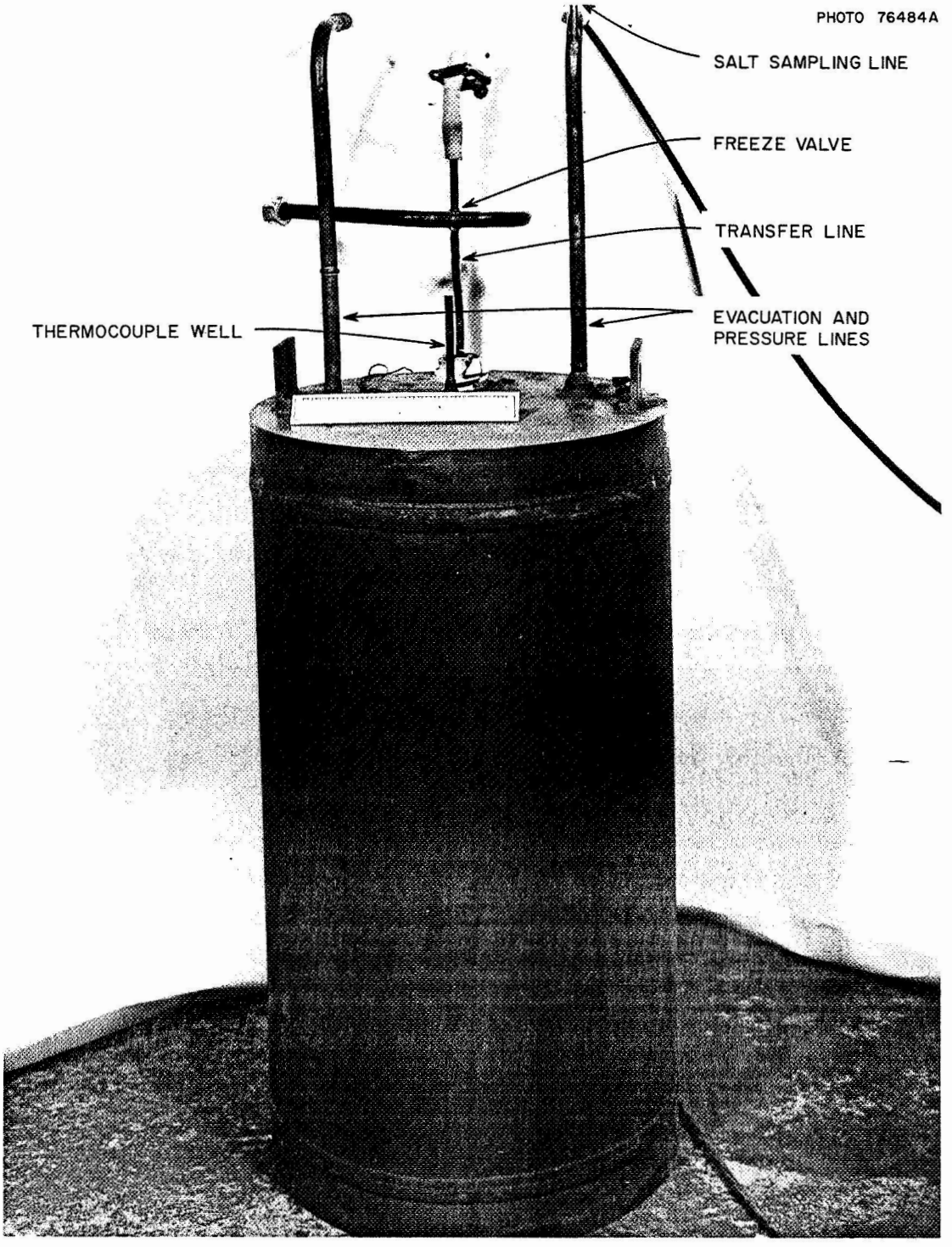

Fig. 18. Salt Reservoir.

The second and third freeze valves had protective loops of unheated 1/4-in. tubing to stop the flow of salt in the event the valves were not completely effective. These protective loops proved helpful, since in some instances the freeze valves were unable to fully stop flowing salt. The cooling medium for these freeze valves was air from the building air supply system.

The chamber evacuation lines were further protected from salt vapors by cold traps. These traps were fabricated from 3-in.-diam 0.065-in.-wall stainless steel pipe and appropriate end caps. The 3-in.-diam pipe was filled with 10 x 10-mesh 0.025-in.-diam stainless steel screen wire.

Preparation of Lithium Fluoride and Loading of Salt Reservoir

Approximately 410 lb of fused lithium fluoride was prepared by the ORNL Reactor Chemistry Division for filling the heat storage tubes and other related purposes. This material successfully met the following chemical purity specifications by weight:

Element	Allowable Impurities (ppm)
S	10
O_2	100
Ni, Cr, and Fe	100
Total	500

The process employed in the purification was essentially the same as that developed for the production of fused fluoride mixtures for ORNL's molten-salt reactor program.[3]

Salt Purification

Fluoride salts of very high purity were purchased commercially and used as the raw materials for the fused fluoride production process. Further purification was required to remove oxides, sulfur, and other halogen impurities and to reduce concentrations of structural metal fluoride impurities that are more noble than constituents of the alloys used in their ultimate containment vessels. Organic impurities were of secondary importance and are normally volatilized during the initial

heatup of the fluorides, or they are thermally decomposed to carbon, which is removed by entrainment in the sparge gas stream or filtered from the molten salt at the conclusion of the purification process.

Anion impurities were removed initially by sparging the molten fluoride with anhydrous hydrogen fluoride. These impurities react directly with the hydrogen fluoride and are conveniently removed from the system as volatile compounds. Research on these reactions, particularly for oxide removal, has shown that high removal efficiencies are attained and that the reactions with hydrogen fluoride proceed essentially to completion.

The ability to reduce certain structural metal impurities in molten fluorides with hydrogen was an important feature of the process. Hydrogen fluoride will readily attack structural metals and alloys that are suitable as salt containers at the operating temperatures of interest by reactions of the type

$$M^{\circ} + 2HF \rightleftarrows MF_2 + H_2 \ .$$

Metal surfaces that are in contact with hydrogen fluoride in the gas phase become passivated by the fluoride corrosion product and are protected from further damage. However, metal surfaces that are in contact with the molten fluoride mixture cannot be protected, since the corrosion film readily dissolves in the melt. Process development studies on the above corrosion reaction with chromium, nickel, and iron have shown that nickel and iron fluorides can be satisfactorily reduced by hydrogen to very low concentrations in molten fluorides at normal operating temperatures of 600 to 800°C. Since chromium and less noble metals are not common impurities in commercial fluoride salts, a simple reduction step with hydrogen to remove iron and nickel sufficed to meet specifications on structural metal impurities.

Development studies have also shown that the corrosion of nickel can be controlled with HF-H_2 gas sparging mixtures that are also effective for oxide, sulfur, and other anion impurity removal from the fluoride mixtures. Accordingly, nickel and other more noble metals are used as liners in stainless steel process equipment for primary salt containment. Since sulfur impurities in fluoride salts are normally present as sulfates, the combination of H_2-HF as a treating gas mixture provides for the continuous reduction of sulfates to sulfides and the volatilization of hydrogen sulfide.

A simplified schematic diagram of the process equipment (2.5-ft^3 batch capacity) is shown in Fig. 19. The starting salt material was loaded directly into the salt treatment vessel and heated under a helium or argon purge to above its melting point (~900°C) with the 50-kw electrical resistance furnace. The melt was then sparged with 10 vol % anhydrous hydrogen fluoride in hydrogen at a flow of about 10 liters H_2 per minute during the initial purification step. Following this treatment the hydrogen fluoride was turned off and the reduction of structural metal fluoride impurities by hydrogen continued. During this period, the salt reservoir was placed in its 27-kw furnace and heated to about 850°C under an inert atmosphere in preparation for filling with the purified fluoride.

Process control was derived primarily from analyses of the gas influent and effluent streams. Samples of the salt mixture were taken periodically under controlled atmospheric conditions for chemical and spectrochemical analyses. When the results of these analyses were below product specifications, the salt was transferred as a liquid through a sintered nickel filter (0.0015-in. pore diameter) into the salt reservoir. Figures 20 and 21 show the operating area of the fluoride production facility and the equipment used in the batch production unit.

Although the batch production facility is normally used for lower melting fluoride mixtures (to 800°C), operating temperatures of 900 to 950°C were conveniently attained for the preparation of pure lithium fluoride. The results of spectrochemical analyses of the starting material indicated the following impurities (by weight):

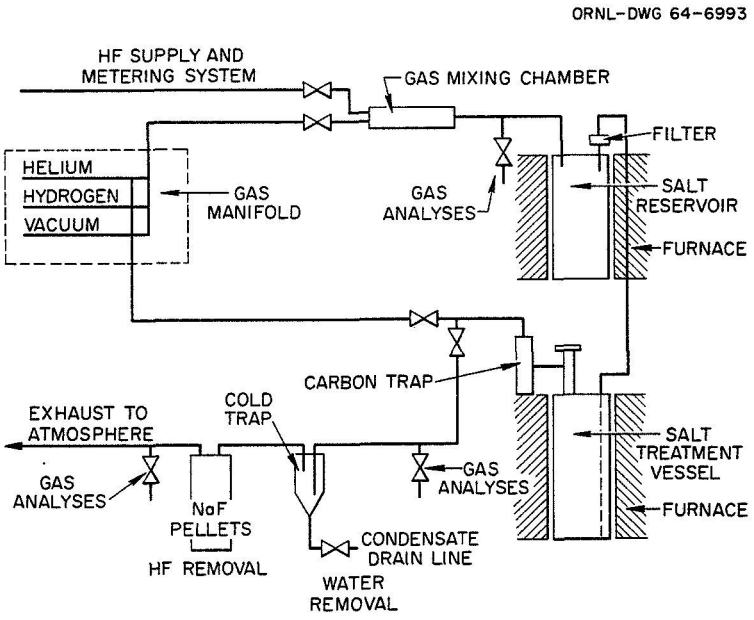

Fig. 19. Simplified Schematic Process Diagram of Fluoride Production Facility.

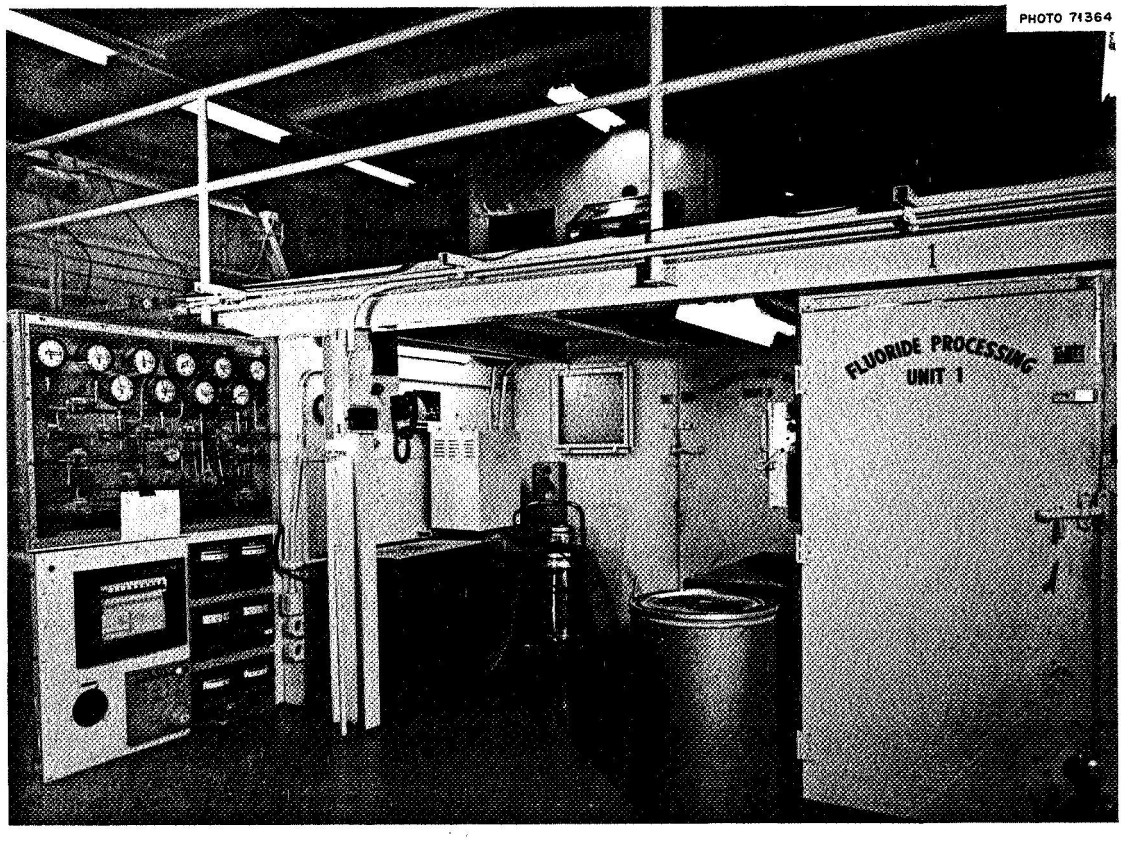

Fig. 20. Operating Floor of Fluoride Production Facility.

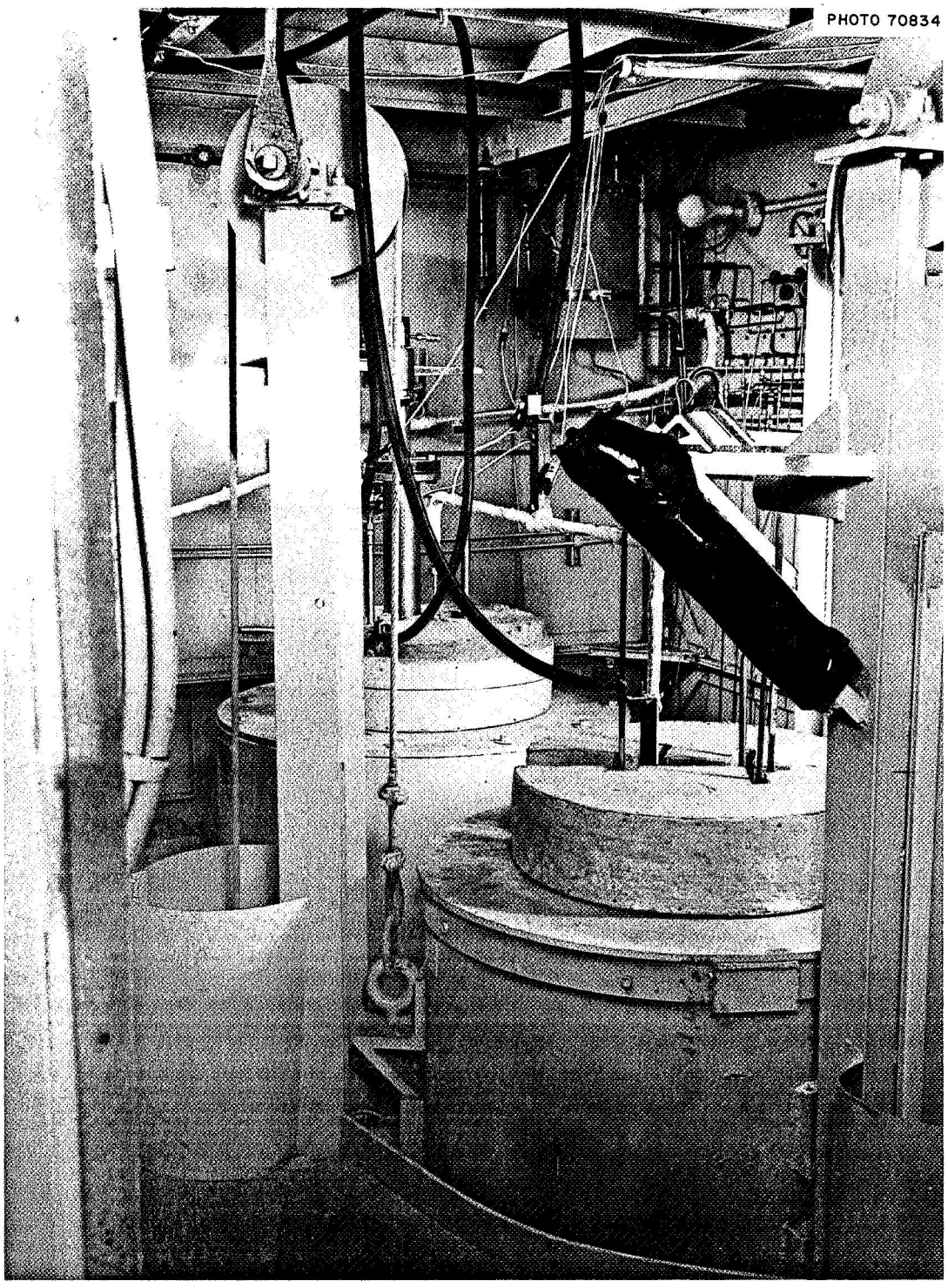

Fig. 21. Fluoride Production Equipment.

Impurity	Content (ppm)	Impurity	Content (ppm)
Ag	<1	Mg	12
Al	<10	Mn	<10
Au	<1	Mo	<1
B	4	Na	<10
Ba	<1	Ni	35
Bi	<2	Pb	<1
Ca	40	Rb	<10
Cd	<2	Si	30
Co	<1	Sn	<2
Cr	1	Ti	<2
Cs	<40	V	<1
Cu	20	W	<40
Fe	25	Zn	<100
K	<6	Sr	<1

Chemical analyses of the material purified by the batch production operation showed the following:

	Content (ppm)	
Impurity	135-lb Batch	275-lb Batch
O	<100	<100
S	<10	<10
Cr	11	37
Fe	18	47
Ni	14	<5

Spectrochemical analyses of the purified material were essentially the same as those for the starting material.

Loading Lithium Fluoride Into the Salt Reservoir

The salt reservoir was designed to contain sufficent material for filling only one set of 15 heat storage tubes. Therefore multiple additions of salt to the salt reservoir from the fluoride production unit were required.

Two methods were used for filling the tank. When the construction schedule allowed, the reservoir was removed from the salt transfer facility and installed in the fluoride production facility. The necessary transfer and gas lines were installed, and two production facility furnaces were used to heat the equipment. After transfer of the lithium fluoride from the production vessel, the salt reservoir was allowed to cool and was reinstalled at the salt transfer facility.

When the construction schedule would not permit this time consuming procedure, the salt was transferred to an intermediate container from the production vessel, and the intermediate container was installed in a portable tube furnace and brought to the salt transfer facility. The portable furnace and the furnace normally used for preheating the salt prior to filling the heat storage tubes were used for heating of the vessels. Both methods were quite successful, and no contamination (as determined by salt analysis) was detected after filling the salt reservoir.

Filling the Heat Storage Tubes

A drawing of the heat storage tubes is shown in Fig. 22. The volume to be filled was the annulus formed by a welded assembly of variable-diameter (2 to 3 1/2 in.) bellows convolutions mounted onto a 1 1/4-in.-OD 1/16-in.-wall tube. The central tube is an argon duct in the Brayton-cycle application. The bellows are nominally 36 in. long and fabricated from 0.030-in. material.

The flowsheet of the filling system was shown in Fig. 3, and an isometric drawing illustrating the physical relationship of the components was presented in Fig. 4.

A protable vacuum pump wagon equipped with a cold trap, a 4-in. diffusion pump, and a roughing pump was used to evacuate the salt reservoir and the filling system. This procedure was necessary to avoid contamination of the heat storage tubes or the salt by contained air or moisture during system heatup.

The initial bakeout of the vacuum chamber and the filling assembly was made at 500°F with the pressure below 1×10^{-7} torr. The pressure tended to increase slightly as temperatures were increased from 500°F; however, continued pumping reduced the pressure to its original value. A rather abrupt change in outgassing rate was noted around 800°F. In order to hold the pressure near 10^{-6} torr, it was sometimes necessary to stop the increase in temperature for several minutes to allow the vacuum pumps to match the outgassing rate.

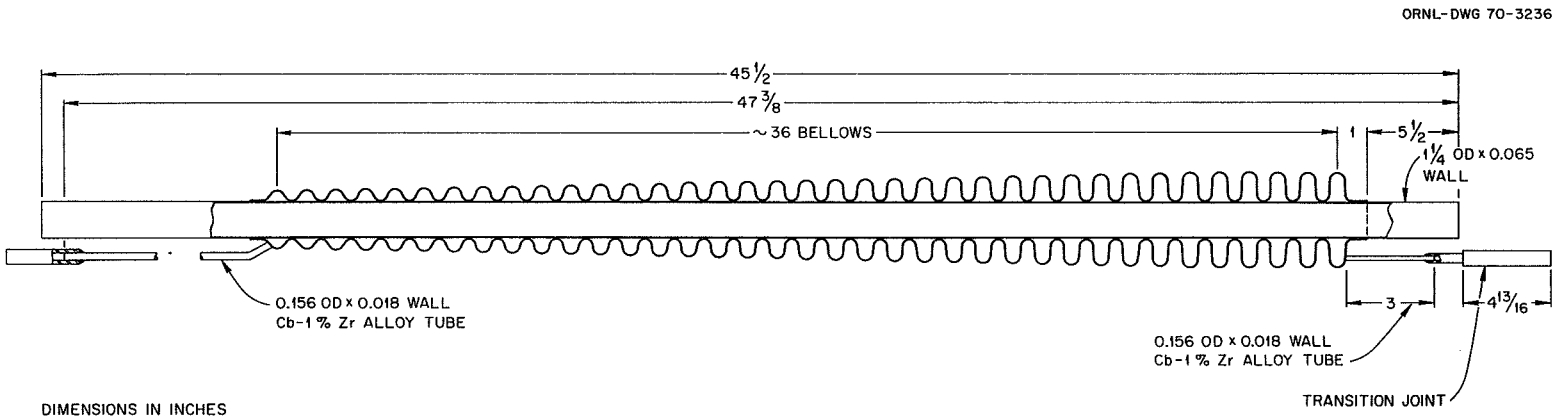

Fig. 22. Heat Storage Tubes.

The pressure was measured at three places in the filling system. Two ion gages were located on the salt reservoir evacuation lines and one ion gage was located on the overflow or vent tank evacuation line. These pressures normally read in the 10^{-4} or 10^{-5} torr range prior to heatup of the tank. After melting they generally were in the 10^{-3} to 10^{-4} torr range. The pressure at the diffusion pump inlet was in the 10^{-5} to 10^{-6} torr range after melting.

After the heat storage tubes and the lithium fluoride had been heated to 1750°F, an overpressure of helium was applied to the top of the salt reservoir. A dip leg in the tank allowed the lithium fluoride to flow upward through the transfer line into a manifold to which 15 of the Brayton-cycle tubes were attached. The filling rate was controlled by a gas restriction installed in the gas line to the salt reservoir. The filling rate was held to less than approximately 0.5 ft^3(STP)/min. This rate allowed the level in the 15 tubes to equilibrate. Normally 20 min was required to fill the tubes after the overpressure was applied to the salt reservoir.

An overflow line at the top of one of the 15 tubes allowed the salt to flow into a sampler. Thermocouples installed on the overflow line (and on the tip of each of the other 14 tubes) gave the indication that the tubes were filled. When the indication of a completed fill was received, a freeze plug was created in the overflow line by passing high-velocity argon around a small section of the line. During the time the freeze plug was being created, a constant overpressure of helium was held on the salt reservoir. Thermocouples on the overflow line at the freeze plug allowed the operators to determine that the freeze plug had been established. Immediately thereafter, freeze plugs were created at the bottom of each of the 15 tubes to trap the correct volume of lithium fluoride in the bellows annulus of the heat storage tubes.

The heater for the heat storage tube assembly was then deenergized and the system allowed to cool. A high-velocity stream of argon was admitted through 3/4-in.-OD conduits installed within the center channels of the heat storage tube configurations. From 10,000 to 12,000 ft^3 of

argon was used to cool each of the filled assemblies. Flow-measuring devices were not installed on the line. The flow rate was controlled by throttling the gas flow to hold the outlet gas temperature to approximately 800°F. The gas was allowed to flow until all the temperatures in the assembly were below 1000°F.

The argon for cooling the freeze valves and for the cooling system for the center of the heat storage tubes was obtained from a building header connected to the Y-12 plant supply. A backup manifold containing fifteen 200-ft^3 cylinders was installed for use in emergencies. Appropriate valving was installed for control to the individual systems.

Some unexpected difficulties with the salt reservoir were encountered during the filling of the heat receiver tubes. A leak occurred in the first tank during preparation for the second filling operation. It was located in the weld where the metallic sheath of a level-measuring device was attached to the salt reservoir head. This leak was small enough and of such a nature that it could be corrected by connecting the externally accessible sheath of the level element to a vacuum pump. Leakage of atmospheric contaminants into the lithium fluoride was thus reduced to an acceptable level.

As a consequence of the leak a decision was made to analyze the salt in the tank prior to the actual filling of the receiver tubes. To expedite the operation, a spectrographic analysis for magnesium was specified as an indication of any possible contamination. Since a large leak would allow migration of MgO insulating material from the level element into the salt, this examination for magnesium would tend to indicate the degree of contamination that might have occurred. The spectrographic analysis gave no indication of an increase of magnesium in the salt, and overflow samples taken at the end of the filling operation also indicated that the salt had not been contaminated by the leak (see Table 7 in following section).

A second leak was detected after four filling operations. This leak was at the same weld but was much larger and could not be tolerated. Since the level element sheath was only 0.010 in. thick and contained compacted MgO insulation, it was felt that the welding operation had weakened the level element wall at the point of attachment. While other vessel welds had been fully inspected, the level element configuration and the weld in question did not lend themselves to complete radiography.

After the tank was disassembled, severe distortion was noted in the dip lines and level probes that had been suspended (see Fig. 23) from the tank top and projected into the lithium fluoride. A 1 1/2-in. pipe that served as protection for the level elements was also slightly bowed. Design reviews indicated that the tank design was adequate for the gas pressures and temperatures during the filling operation; however, the design did not accommodate the unexpected forces encountered during melting of the lithium fluoride. The origin of these forces is not thoroughly understood. One theory explains them as being generated by a piston effect that occurred when the contents of the tank were melted from the bottom upward. Another theory explains the forces as being due to differences in expansion coefficients in the lithium fluoride and container material. More information on salt characteristics at or around the melting point and more experience with lithium fluoride would be required for an exact explanation.

Examination of the columbium–1% zirconium foil installed inside the tank as gettering material revealed some embrittlement at the top of the three outside layers. Analysis of the embrittled foil revealed considerable pickup of oxygen and nitrogen. Exposed foil showed 5300 ppm of oxygen compared with 300 ppm in the unexposed foil and 1400 ppm of nitrogen compared with 140 ppm in the unexposed foil. The inner layers were less affected and thus were quite ductile. The columbium–1% zirconium material was to some extent effective in gettering the oxygen and nitrogen that entered the tank during the leak; however, no attempt was made to analyze the lithium fluoride for residual contaminants before it was discarded.

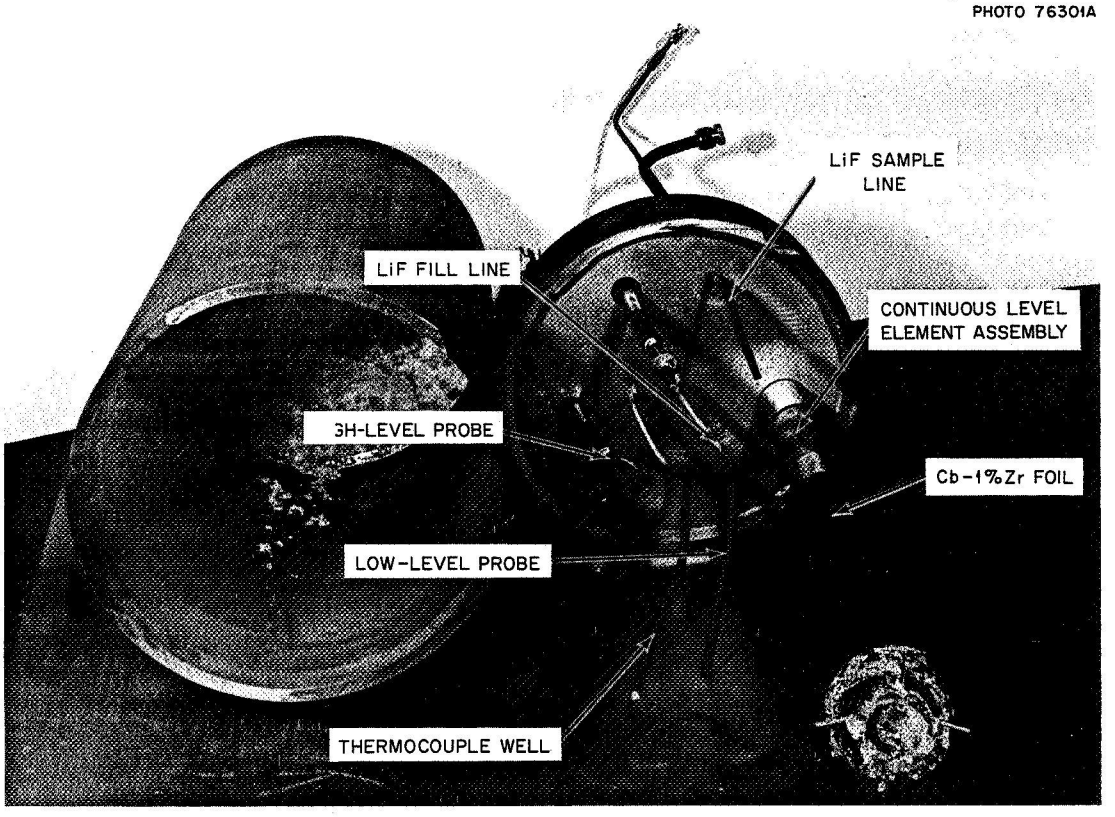

Fig. 23. Salt Reservoir Showing Distortion of Lines Inside Tank.

A second salt reservoir was fabricated after the design was changed to omit the level elements. The new tank was installed and a fifth filling operation was accomplished. During the heatup operation for the sixth and final filling operation, a leak developed in this tank. The leak occurred just as the salt reached the melting point (~1560°F), and atmospheric air entered the evacuated heat receiver tubes and the fill tank.

This leak occurred at the weld adapter through which the transfer line penetrates the fill tank. The thin lip of the adapter to which the fill line is welded had been torn and separated approximately 3/16 in. This failure too was attributable to the upward forces exerted on the fill line during melting of the lithium fluoride, although extreme care had been exercised in controlling heating and melting rates to avoid this problem. The accumulative effect of these forces during the four heatup operations necessary to the fifth and sixth filling operations was probably the cause of the failure.

The heat storage tube assembly had been heated to between 1250 and 1450°F when the leak developed, and the pressure in the annulus of the tubes had increased to approximately 128 μ. The electric power to the furnace was immediately deenergized; however, the temperatures did not cool to 800°F until 3 hr later and to 500°F until a total of 8 hr had elapsed.

One of the storage tubes was removed from the assembly, and metallographic examinations were made to determine the amount of contamination that had occurred. The results of this examination are shown in Fig. 24.

The bellows material analysis showed a maximum of 240 ppm of oxygen in the columbium–1% zirconium material. The contamination received during the leak incident was considerably less, however, since the material used for the bellows assembly was obtained from one of two lots that showed initial values of 80 to 150 ppm. Assembly welding and heat treating of the completed tubes may have added to these "as-received" values.

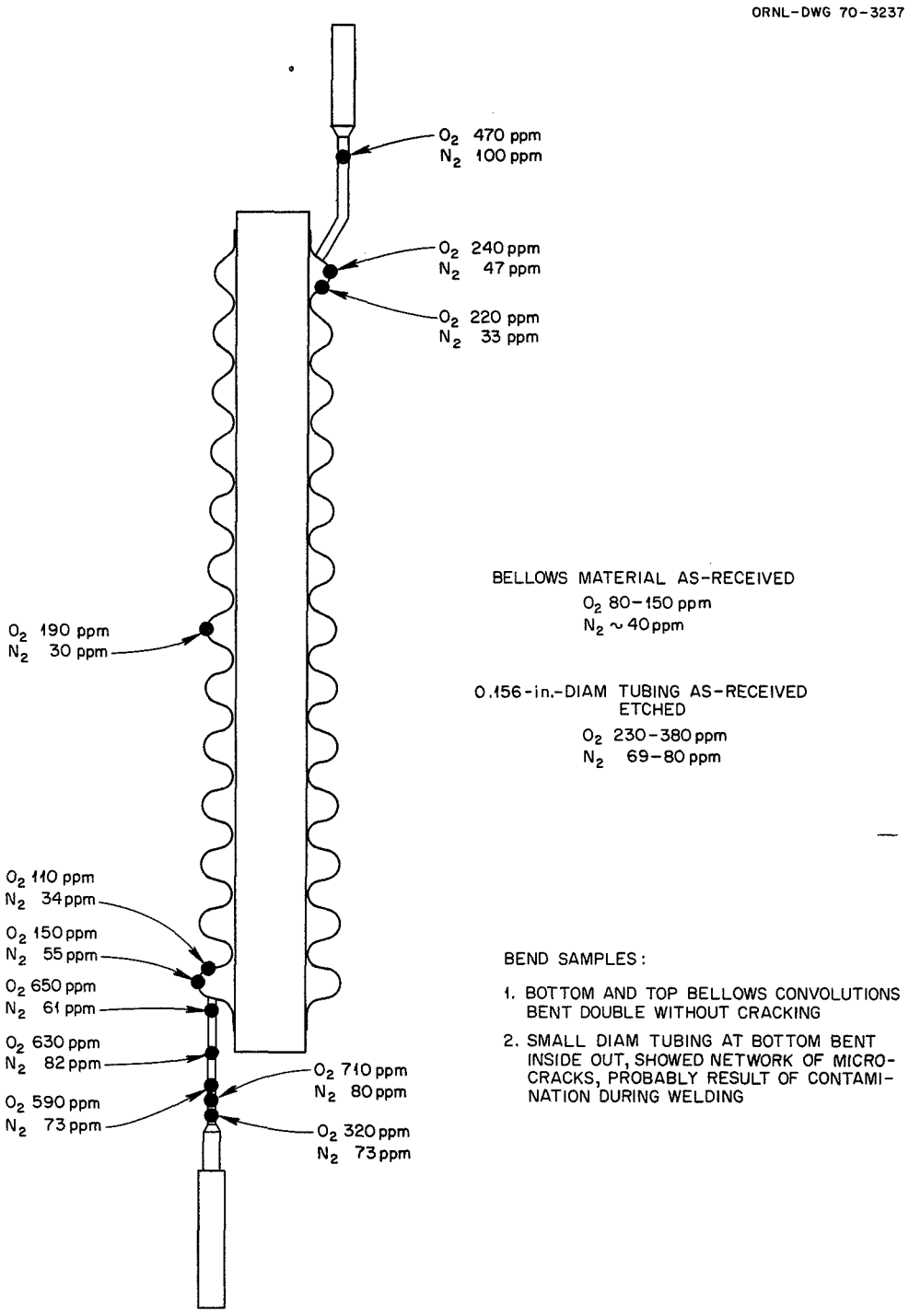

Fig. 24. Results of Analyses of a Columbium–1% Zirconium Heat Storage Tube After Aborted Sixth Filling Operation.

The fill and vent connections to the bellows (0.156-in.-OD x 0.018-in.-wall tubing) showed rather high gross oxygen content. The values of 470 and 630 ppm were of concern; however, earlier analysis had shown that this particular material contained from 230 to 380 ppm of oxygen when received. This material was obtained by the NASA Lewis Laboratory from CANEL material declared surplus by the Pratt & Whitney Company. Chemical analyses of various pieces of this CANEL material indicated that the oxygen content varied considerably. Microscopic examination also indicated that the method of forming this material had left microscopic grooves on the inner surface of the tubing and a dark material in the grooves. These deposits evidently were not completely removed by etching, since earlier weld examination had disclosed that the inner surface of the tubing near the weld area was oxygen contaminated to some extent, while the outer surface of the tubing did not show contamination.

It is quite doubtful that the total increase from 230 to 380 ppm to 540 to 630 ppm of oxygen for these small tubes was due to contamination by the leak in the fill tank. Some of the contamination probably occurred during welding of the tube assemblies.

Specimens taken from the 0.156-in.-OD tubing withstood bend tests without evidence of brittle cracking; however, microscopic examination of the inner surface disclosed a network of microcracks. Bend tests were also made on the bellows material, and there was no evidence of embrittlement.

The lithium fluoride in the fill tank was badly contaminated, and it was necessary to purify new salt for filling the remaining tubes. The contaminated salt was removed from the reservoir, and new weld adapters for line penetrations were designed, fabricated, and installed. An expansion loop was also designed and installed inside the tank for all tank penetrations to reduce the thrust loads on the tank penetration nozzles during melting of the lithium fluoride. After the modifications to the reservoir had been made and a new salt charge added, the sixth filling operation was completed without further incident.

During the heatup operation for filling the third group of 15 tubes a leak developed in the sheath of a 1/16-in.-diam thermocouple installed inside the heat storage tube assembly. A quick cooldown was immediately instigated to protect these tubes from oxygen contamination. The leak rate through the thermocouple was small enough that the vacuum pressures of the chamber never exceeded 1×10^{-5} torr. After the fast cooldown a second leak was discovered in one of the freeze valve welds in the assembly that was probably due to high stresses generated during the thermal transient. This weld was repaired; the damaged thermocouple was replaced; the assembly was reinstalled in the vacuum chamber; and the filling operation was completed.

Disassembly of Filling Facility and Plugging of Heat Storage Tubes

After the filling operation, the facility was moved to the controlled access room for disassembly. The filled heat storage tubes were weighed and x-rayed to determine the content of lithium fluoride and to check the freeze pattern of the salt. The results are discussed in the following section.

Salt was removed from the fill and vent tubes by reaming with a 0.116-in.-diam drill. The drill, which was driven by a slow-speed drill motor, broke the salt crystals from the inner surface of the tube. Extreme care was necessary during this operation to assure that the walls of the fill and vent tubes were not damaged. Subsequent cleaning operations consisted of scraping with a small stainless steel blade and wiping with an ethyl alcohol-soaked nylon cloth.

Each 0.156-in. tube was then cut to a 3/4-in. length, argon was purged into the opening, and shrink tubing was installed over the open end of the tube to prevent exposure to the atmosphere.

A weld design to plug the ends of the fill and vent tubes was developed (Fig. 25), and a tightly fitted columbium–1% zirconium plug was installed in the end of each tube and electron-beam seal welded as shown in Fig. 26. Photomicrographs of test welds disclosed that the weld technique was quite satisfactory. X-rays were taken of all plug welds and examined for fusion, penetration, and porosity.

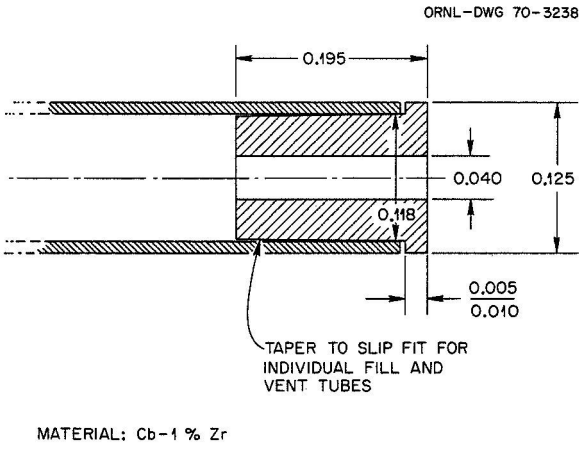

Fig. 25. Weld Design for Plugging Ends of Fill and Vent Tubes.

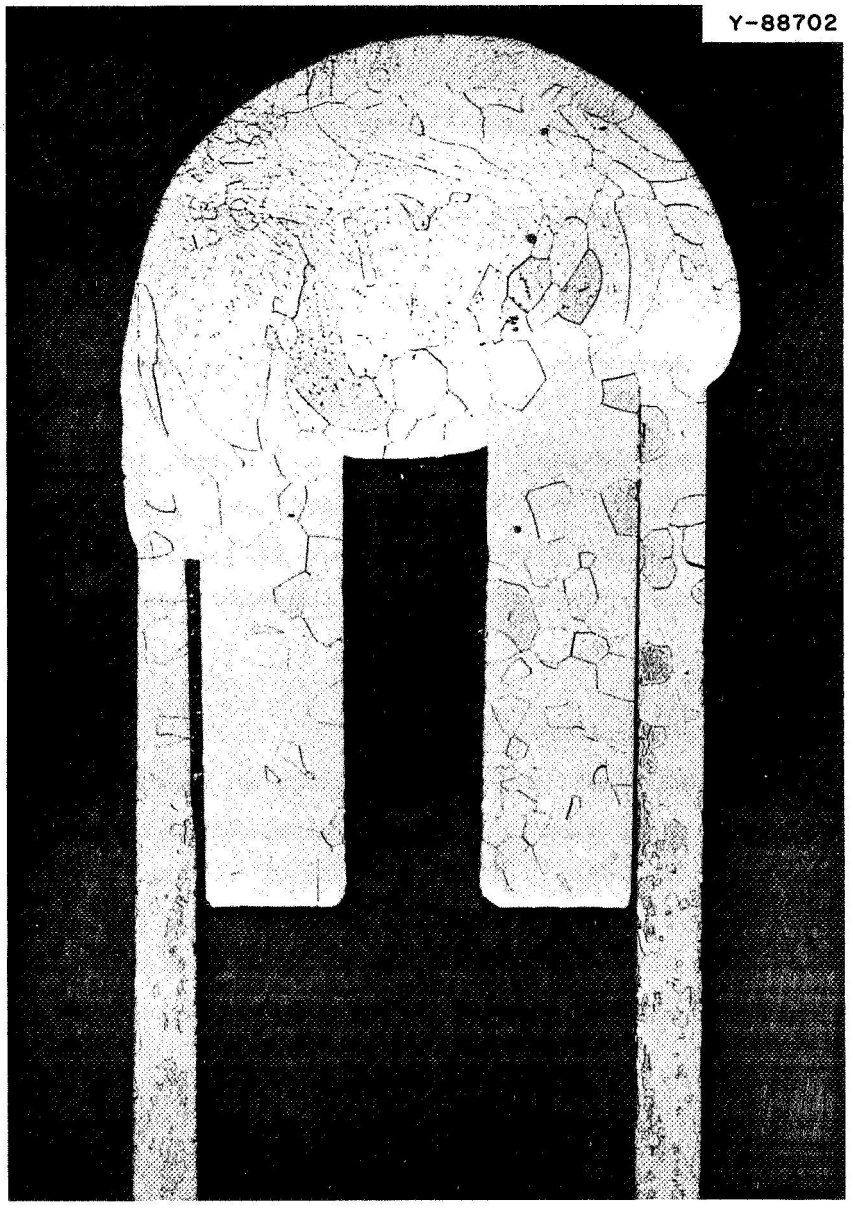

Fig. 26. Photomicrograph of Plug Weld of a Fill Tube.

The electron-beam seal welds were made on a 6-kw Hamilton Standard Electron Beam Welder, Model W-2. The chamber of the welding facility was evacuated to a minimum 1×10^{-5} torr prior to the welding operation. Pumping times of approximately 2 hr at this minimum pressure seemed to result in fewer weld rejections. Beam power settings of 80 kv and 6 ma were used. The beam was swept linearly at right angles to the tube axis, with an amplitude of approximately 1/4 in. It initially impinged on a tungsten block, and then the tube end was manually fed into the beam until the required amount of melting was visually observed. A schematic diagram of the equipment is shown in Fig. 27.

The weld integrity was sensitive to operator technique, and practice welds were required before the final closure welds were made on the assemblies. In some instances microscopic salt particles were inadvertently left on the inner surface of the tube wall, and heating of the salt caused blowouts and porosity. In every instance of weld rejection it was possible to repair faulty welds by refusing the weld bead or replugging and rewelding.

Results of Filling Operations

The filling technique was first checked by filling an 11-convolution stainless steel tube in air. Subsequent fills of columbium-1% zirconium tubes in the vacuum chamber included filling one tube of 11 convolutions, filling a nine-tube assembly containing six standard tubes and three shortened tubes, and filling four 15-tube assemblies. Data on the tubes filled in the vacuum chamber and their salt contents are presented in Tables 1 through 5.

Examination of x-rays of the heat storage tubes after filling indicated that the tubes had been satisfactorily filled. A freeze plug was properly formed at the 0.005-in. annulus between the bottom of the bellows convolutions and the outside wall of the 1 1/4-in. center conduit, since the lithium fluoride distribution was such that a void was apparent in all but the top convolutions. X-rays of a portion of a typical tube before and after filling are shown in Fig. 28.

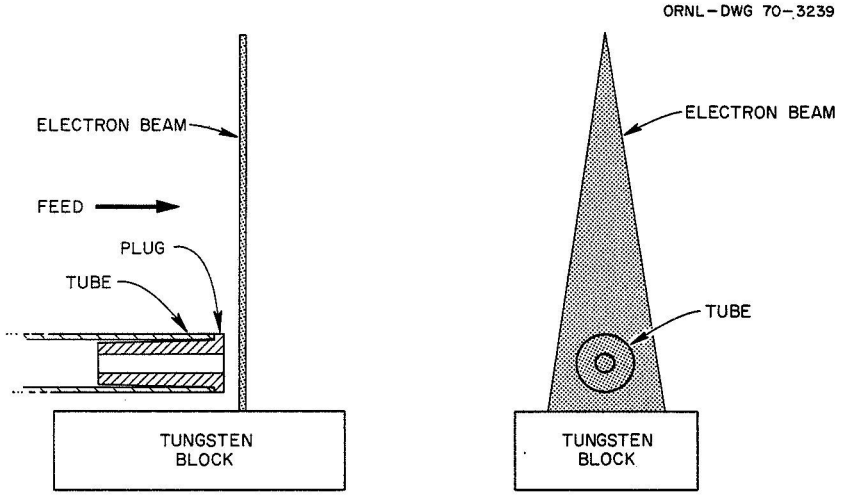

Fig. 27. Electron-Beam Welding Technique.

Table 1. Weights and Volumes of First Ten Heat Storage Tubes

Tube No.	Gas Volume at Room Temperature (cm^3)	Tube Weight (g)		LiF Added (g)	Calculated LiF Content at Room Temperature (g)
		Before Filling	After Filling		
2,[a] 82	1423	2809	5385	2576	2492
3, 10	1410	2809	5358	2549	2469
4, 24	1453	2820	5422	2602	2544
5, 31	1340	3493	5900	2408	2346
6, 48, 97	1334	3474	5883	2409	2336
23	611	1569	2697	1128	1070
30	622	1583	2701	1118	1089
1, 62	1436	2785	5337	2552	2514
90	620	1682	2789	1108	1086
___[b]	656			1173	1149

[a]Not same tube as tube 2 in Table 2.

[b]First tube filled; not numbered.

Table 2. Weights and Volumes of Heat Storage Tubes Filled in Run 15-1

Tube No.	Gas Volume at Room Temperature (cm^3)	Tube Weight (g)		LiF Added (g)	Calculated LiF Content at Room Temperature (g)
		Before Filling	After Filling		
2	1393	2759	5275	2516	2439
7	1406	2736	5254	2518	2462
8	1408	2760	5270	2510	2465
11	1404	2752	5276	2524	2458
13	1396	2706	5228	2522	2444
14	1399	2730	5238	2508	2450
40	1399	2719	5239	2520	2450
43	1409	2751	5266	2515	2467
51	1410	2774	5329	2555	2469
60	1396	2757	5274	2517	2444
81	1393	2743	5258	2515	2439
91	1398	2760	5280	2520	2448
94	1412	2823	5364	2541	2472
98	1405	2759	5272	2513	2460
101	1398	2767	5286	2519	2448

Table 3. Weights and Volumes of Heat Storage Tubes Filled in Run 15-2

Tube No.	Gas Volume at Room Temperature (cm^3)	Tube Weight (g)		LiF Added (g)	Calculated LiF Content at Room Temperature (g)
		Before Filling	After Filling		
1-5	1397	2735	5250	2515	2446
1-7	1379	2731	5254	2523	2414
1-8[a]	1396	2747	5277	2530	2444
1-9	1395	2745	5272	2527	2443
1-10	1388	2759	5286	2527	2430
1-12	1398	2744	5262	2518	2448
1-14	1401	2734	5260	2526	2453
1-20	1389	2732	5279	2547	2432
1-21	1387	2748	5267	2519	2429
1-23	1393	2742	5261	2519	2439
1-31	1380	2749	5265	2516	2416
2-1	1398	2767	5288	2521	2448
2-8	1398	2820	5343	2523	2448
51-A	1396	2796	5317	2521	2444
54-A	1388	2819	5335	2516	2430

[a]Overflow tube attached to this heat storage tube.

Table 4. Weights and Volumes of Heat Storage Tubes Filled in Run 15-3

Tube No.	Gas Volume at Room Temperature (cm^3)	Tube Weight (g)		LiF Added (g)	Calculated LiF Content at Room Temperature (g)
		Before Filling	After Filling		
2-2	1405	2779	5302	2522	2460
2-4	1387	2737	5257	2520	2429
2-6	1397	2748	5268	2520	2446
2-7	1388	2771	5288	2517	2430
2-9	1396	2768	5282	2514	2444
2-13	1390	2769	5283	2514	2434
2-14	1402	2781	5300	2519	2455
2-16	1401	2750	5268	2518	2453
2-17	1400	2773	5292	2519	2451
2-19	1401	2759	5278	2519	2453
2-25	1400	2743	5266	2523	2451
2-26	1403	2756	5275	2519	2457
2-27[a]	1402	2830	5353	2523	2455
52-A	1391	2791	5313	2522	2436
53-A	1403	2800	5325	2525	2457

[a]Overflow tube attached to this heat storage tube.

Table 5. Weights and Volumes of Heat Storage Tubes Filled in Run 15-4

Tube No.	Gas Volume at Room Temperature (cm^3)	Tube Weight (g)		LiF Added (g)	Calculated LiF Content at Room Temperature (g)
		Before Filling	After Filling		
2-3	1419	2723	5251	2528	2485
2-5	1426	2685	5232	2547	2497
2-11	1417	2688	5238	2550	2481
3-1	1422	2733	5291	2558	2490
3-4	1424	2743	5296	2553	2493
3-7	1411	2731	5273	2542	2471
3-8	1409	2737	5285	2548	2467
3-9	1414	2727	Removed for examination after aborted fill operation		
3-14[a]	1431	2835	5379	2544	2506
3-15	1410	2697	5245	2548	2469
3-16	1427	2695	5249	2554	2499
3-17	1428	2684	5232	2548	2500
3-18	1415	2719	5263	2544	2478
3-24	1414	2737	5285	2548	2476
3-28	1424	2720	5255	2535	2493

[a]Overflow tube attached to this heat storage tube.

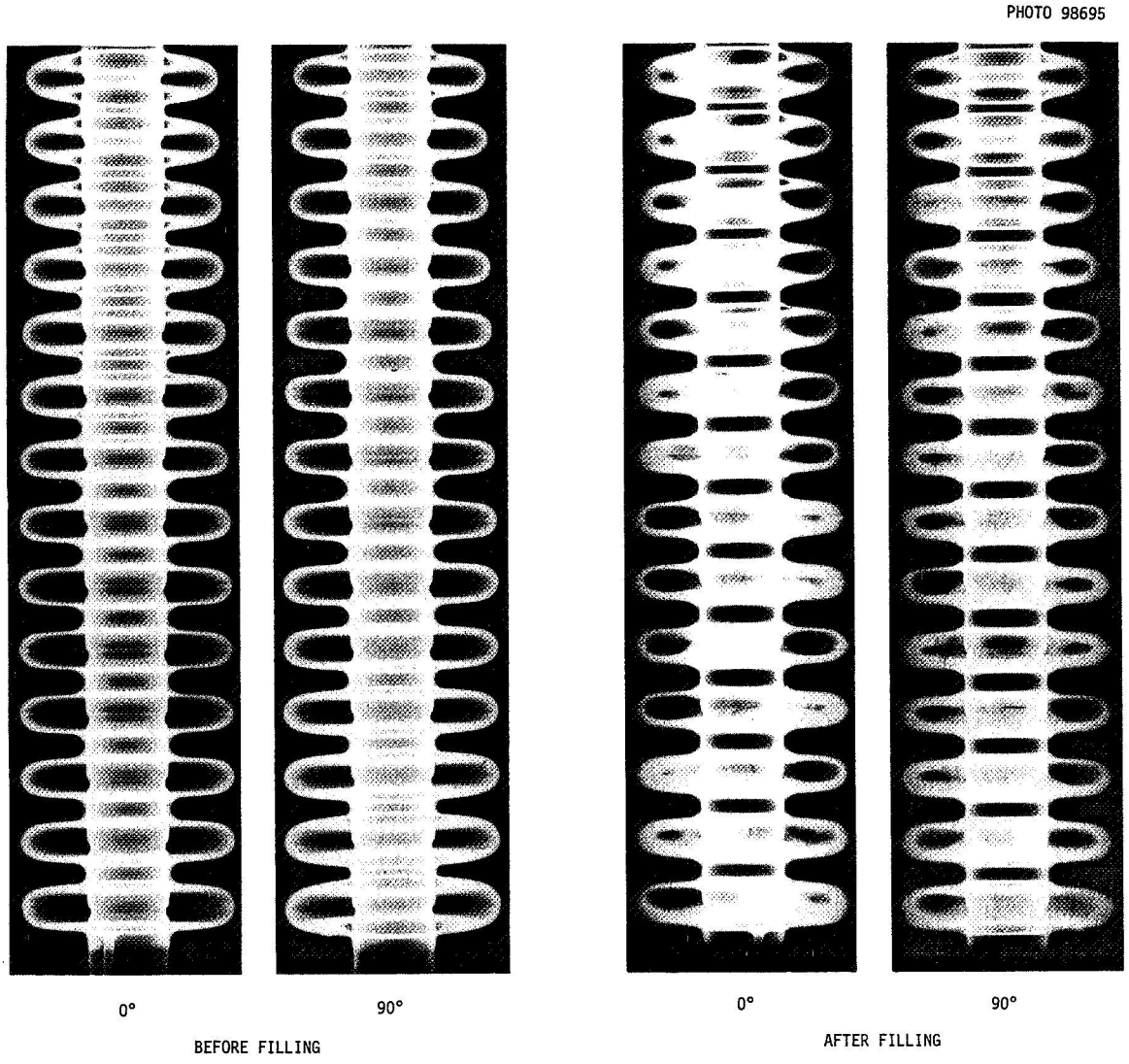

Fig. 28. X-Rays of Heat Storage Tubes.

The x-rays indicated that the two top convolutions did not contain a proportionate amount of lithium fluoride. Since thermocouples installed on each of the vent tubes at the top of each heat storage tube had indicated that salt actually had filled the tubes completely, investigations were undertaken to determine why these two top convolutions were not properly filled.

Special x-ray techniques were used to determine that lithium fluoride had coated the inner bellows walls. Physical examination (probing with a small stainless steel wire) through the 0.120-in. opening in the vent tube also disclosed that some salt was clinging to the walls. However, the freeze pattern shown by the x-rays was not the same as for the lower convolutions. Speculation on the reason for the lower salt content in the top convolutions centers around the temperature profiles within the convolutions during the process of cooling from 1750°F, the filling temperature, to 1560°F, the freezing temperature. The more gradual the cooling the more uniform the temperature would be across the salt cross section. The limiting case of a flat temperature profile would result in an approximate 2% density change over this temperature range and a salt volumetric contraction of 1.7 $in.^3$. Such an event would have essentially emptied the approximate 1.8-$in.^3$ volume of the top two convolutions before freeze seals were formed between the other convolutions to prevent further salt movement. Although the actual cases could not have been this severe, the lower salt inventory in the top two convolutions was obviously caused by this mechanism.

X-ray examinations of the top convolutions on the tubes to which the overflow lines were attached (one in each 15-tube assembly) indicated that these tubes contained disproportionately large amounts of lithium fluoride and that the freeze pattern was again different. The overflow line extended in a 7-in.-diam 90° arc to a point approximately 4 in. above the top convolution. It is postulated that when the freeze plug was created at the high point in the overflow line, some of the salt in this line flowed back into the top convolution before freezing occurred.

The amount of backflow could not be accurately measured; however, the void volume in the overflow line in each case was very small (~0.1 in.^{3}). Since the average volume of the top convolution was estimated to be 0.894 in.^{3}, the backflow was not considered serious.

Columbium–1% zirconium coupons were placed in the vacuum chamber with each of the tube assemblies. These coupons were analyzed by vacuum fusion analysis after each filling operation, and the results were compared against standards. The difference in these results was used to determine the amount of oxygen, nitrogen, and hydrogen contamination that occurred during the filling operation. Table 6 lists the measured contamination values.

Table 6. Contamination[a] of Columbium–1% Zirconium Coupons Installed in Assembly Fixture

Fill Run	Contamination (ppm)		
	H_2	N_2	O_2
1 tube	4	30	120
9 tube	>1	2	80
15-1	>1	10	30
15-2	5	0	50
15-3	0	0	>100
15-4	0	0	>140

[a] Determined by difference in analytical values before and after exposure.

Salt samples were taken for analysis at various intervals during the filling of the heat storage tubes, and an overflow sample was taken after each filling operation. Results of analyses of the overflow samples are given in Table 7.

Table 7. Results of Analyses of Lithium Fluoride Samples Taken from Overflow Lines

Fill Run	Elemental Impurities (ppm)				
	N_1	Cr	Fe	O_2	S
1 tube	14	11	18	100	8
9 tube	~3	20	3	94	
15-1	>5	16	104	57	9
15-2	>25	34	81	>50	
15-3	>8	12	28	>25	
15-4	10	25	23	123	

References

1. D. T. Bernatowicz, NASA Brayton Cycle Studies, NASA Lewis Technical Preprint 13-63, September 1963.

2. Donald Q. Kern, Process Heat Transfer, p 76, McGraw-Hill, New York, April 1950.

3. Oak Ridge National Laboratory, Reactor Chemistry Division Annual Progress Report for Period Ending January 31, 1965, USAEC Report ORNL-3789, p 99.

APPENDICES

Appendix A

LIST OF FILLING FACILITY DRAWINGS

Drawing No.	Revision No.	Title
		Mechanical
10454-R-001-E	2	General Assembly P/L & Plain View
002-E	2	General Assembly, Elevation Section
003-E	1	Insulation Details
004-E	1	Insulation Details
005-E	0	Insulation Cylinder-Details and Assembly
006-E	1	Support Ring Weldment
007-E	1	Heater Assembly
008-E	1	Support Stand Weldment
009-E	1	Centering Post Weldment
010-D	1	Capsule Assembly
011-E	3	LiF Freeze Valve Manifold S.A.
012-E	1	Cooling Manifold Details
013-E	1	Details
014-E	3	Drain & Fill Tank Weldment, Sh. 1
015-E	2	Vent Tank Weldment
016-E	2	Level & On-Off Probes
017-E	1	LiF & Argon Penetrations
018-E	1	Drain & Fill Weldment Details
019-E	0	Vent Tank Support Assembly & Details
020-E	5	Gen. Arrangement Ext. Piping
021-E	1	Details
022-E	5	Drain & Fill Tank Weldment Sh. 2
B-SK-4203 B	E	Flow Diagram
A-SK-4202 C	A	Transition Joint
A-SK-4404 0	A	Lava Bushings
		Electrical
10454-R-501-E	1	Schematic Diagram, Power System Sh. 1
502-E	1	Assembly & Wiring, Control Cab. No. 3
503-D	1	Control Panel, Front Elevation & Plan
504-D	1	Assembly & Wiring, Control Cab. No. 4
505-D	1	Assembly & Wiring, Control Cab. No. 5
506-E	0	Assembly & Wiring, Control Cab. No. 8
507-D	1	Assembly & Wiring, Control Cab. No. 2
508-D	0	Assembly & Wiring, Control Cab. No. 1
509-D	0	Assembly & Wiring, Control Cab. No. 6
510-E	1	Thermocouple Layout, Fill Fixture
511-E	2	Schem. Diagram, Power System, Sh. No. 3
500-E	2	Heater & Thermocouple Layout
1-10454- 001-D	0	Control Cab. No. 7, Panel Layout

LIST OF FILLING FACILITY DRAWINGS (cont'd)

1-10454-002-D	0	Control Cab. No. 7, Wiring Table
003-D	0	Control Cab. No. 7, Wiring Table
004-D	0	Stokes Vacuum Control Cab. No. 1, Wiring
005-D	0	Vacuum System, Maintenance Schem.
006-D	0	Vacuum System, Maintenance Schem.
007-D	0	Vacuum System, Maintenance Schem.
008-D	0	Vacuum System, Annunciator Wiring
009-E	0	Vacuum System, Instrument Flow Diagram

Appendix B

RECORD OF DESIGN REVIEW AND APPROVAL BY ORNL PRESSURE VESSEL AND PIPING REVIEW COMMITTEE

cy to PAGnadt/fr. EJB/6-22-67

INTRA-LABORATORY CORRESPONDENCE

OAK RIDGE NATIONAL LABORATORY

June 21, 1967

PR-19

To: E. J. Breeding

Subject: Hastelloy N – Inconel Vessel – Drain and Fill Tank, Drawing 10454R-014-E

The drain and fill tank consisting of a 3/8" "Hastelloy-N" shell welded to two flat 2-in.-thick "Inconel-600" heads has been reviewed for operation at 15 psi and 1800°F for an estimated lifetime of 100 hours.

The temperature is beyond the maximum for either material given in Section VIII of the ASME Boiler and Pressure Vessel Code. Allowable stresses were determined for "Inconel-600" using the Code basis for establishing stress values and data contained in Inco Technical Bulletin T-7. The maximum allowable stress for 1800°F was found to be 340 psi based on 0.1% creep per 10,000 hours. The head's thickness is adequate for this allowable stress.

Available data for "Hastelloy-N" indicate the allowable stress as determined using the Code basis would not be adequate for this vessel. Data reported in ORNL-4037, "Molten-Salt Reactor Program Semiannual Progress Report for Period Ending August 31, 1966," for 100 hours indicates a stress rupture value of 3,300 psi and a creep rate of 1% at 1500 psi. Since the calculated stress in the shell is 250 psi, it is felt that the vessel will operate satisfactorily at the design conditions for the 100-hour lifetime.

I have discussed the possibility of "catastrophic oxidation" of the "Hastelloy-N" with B. Fleisher of the M&C Division and have been assured this will not be a problem.

C. W. Collins

C. W. Collins

CWC:lf

cc: C. J. Claffey
B. Fleisher
W. R. Gall
M. I. Lundin
H. A. Nelms
T. W. Pickel
G. C. Robinson
J. N. Robinson
R. W. Schneider
CWC file

INTRA-LABORATORY CORRESPONDENCE

OAK RIDGE NATIONAL LABORATORY

January 29, 1969

To: P. A. Gnadt

From: C. W. Collins

Subject: Pressure Vessel Review No. 44
Filling Facility for NASA Capsules

The piping flexibility calculations performed by T. E. Haynes were reviewed for compliance with the "Code for Pressure Piping," ASA B31.1, and SPP-12B.

The facility consists of tubing manifolds, cooling system and freeze valves which are contained in a vacuum vessel that isolates the system from the atmosphere and operating personnel. Materials used in the facility include stainless steel, Inconel, Hastelloy-N and columbium operating at essentially zero pressure and temperatures up to 1775°F.

The highest stress due to thermal expansion in the system occurred in a Hastelloy-N tube which undergoes 5 cycles of stress calculated to be 103,000 psi. Although this exceeds the Code allowable stress by a considerable amount, data given by A. E. Carden in ASME Paper No. 64-MET.-2 indicates this material would have a fatigue life of about 100 cycles for this stress at 1600°F.

Even after making some allowance for operating at 1775°F rather than 1600°F, it is felt the component having the highest stress would have a fatigue life greater than the required 5 cycles. This particular component can be examined after each cycle so that it could be replaced if there is undue distortion and is contained in the vacuum vessel so there is no hazard to operating personnel.

C. W. Collins

CWC:lf

Copy to:
S. E. Beall
C. J. Claffey
W. R. Gall
T. E. Haynes
M. I. Lundin
R. E. MacPherson
H. A. Nelms
G. W. Renfro
G. C. Robinson
A. F. Zulliger
File (CWC)

Appendix C

DRY-BOX PROCEDURE FOR WELDING HEAT STORAGE TUBES

1. All material (except the 0.156-in. tubes attached to bellows assemblies) is cleaned in accordance with cleaning procedure.
2. Box is pumped to approximately 0.05 μ (0.00005 mm Hg).
3. Leak-up rate is established at less than 30 to 35 μ/hr.
4. Box is purged to atmospheric pressure with argon. Typical gas analysis (vol %) is:

H_2	0.0004
H_2O	0.0005
N_2	0.0013
O_2	0.0001
CO_2	0.001

5. An arc is struck on titanium or zirconium block for gettering; also indicates purge gas purity.
6. A 1/8-in. weld pass is made on a coupon of stainless steel. A very light straw color on the stainless steel indicates that the oxygen and moisture levels are below 5 ppm.
7. Test weld is made on columbium–1% zirconium sheet. Discoloration is normal guide to atmosphere contamination. Bend test is made on test specimen but not always prior to welding parts.
8. Parts are welded.
9. Test weld is made on columbium–1% zirconium sheet and checked for discoloration.
10. Welds are dye checked and x-rayed.

Appendix D

HEAT STORAGE TUBE FABRICATION AND ASSEMBLY

Cleaning of Inconel, INOR-8, and Stainless Steel

Solvents--trichloroethylene, perchloroethylene, acetone, and ethyl alcohol shall be used for degreasing. A clean white cloth saturated with solvent may be used to wipe parts. It is especially important that oxide from welding be prevented or removed, if possible, by stainless steel brushing or other approved methods from all parts and subassemblies that cannot be reached for direct inspection and cleaning after assembly. Vapor blasting (liquid honing) using aluminum oxide abrasive may be used to remove ink markings, surface oxide, and foreign materials. After cleaning, all abrasive shall be removed from each component with water or steam and one or more of the solvents listed above.

Pipe and tube shall be cleaned by forcing hot tri-sodium phosphate, steam, and dry nitrogen through the inside of each tube in the manner presently used at ORNL for cleaning piping. A description of cleaning procedures at the 7000 Area Cleaning Facility is attached for reference.

Discoloration of surgical gauze after wiping metal surfaces shall be used as a check for cleanliness.

Compounds containing sulphur, lead, aluminum, zinc, or mercury shall not be permitted to come into contact with surfaces of material.

I. Description of Cleaning Procedures at the 7000 Area Cleaning Facility (ORNL)*

Upon receipt of material at the Cleaning Facility, it is visually inspected for cleanliness. If grease, oil, or dirt is present, the material is washed with acetone, hot water, or blown with air to remove the excess.

*From a memo to F. T. Anderson from E. W. Parrish dated March 28, 1957.

The material is then lowered into a vat of five percent trisodium phosphate (100 pounds of technical grade TSP to 280 gallons potable water) at 80°C. This solution is circulated through the vat at 60 gallons per minute. The inlet line is arranged so as to allow maximum flow through pipe being cleaned. The material is to remain in this solution for one half hour minimum.

The material is then lowered into a vat of cold potable water. The potable water flows through the vat at 50 gallons per minute and is continuously discharged to waste. The material is rinsed in this vat for one half hour.

The material is then lowered into a vat of hot circulated potable water (80°C) at 20 gpm for one half hour. It is then removed to a rack where it is air dried with 90°C filtered air.

The material is then finally inspected for cleanliness and remarked if the identification was removed during cleaning. A rubber stamp and approved marking ink is used for remarking. Pipe is to be marked on twelve inch (12 in.) centers.

Packaging materials currently being used are:

(a) Pipe-ends are covered with plastic film with masking tape over the plastic. Plastic caps will be used when available.

(b) Fittings and small parts - Plastic bags wired closed.

(c) Large materials - Plastic.

II. Operating and Sample Log

All materials that pass through the Cleaning Facility are logged in and out. The following information is recorded in the operating log:

(a) Inspection request or store stock item number of the material.

(b) Description of material.

(c) Quantity of material.

(d) Date cleaned.

(e) Type cleaning.

(f) Cleaning solution and rinse sample numbers.

(g) Records are maintained on the date that the cleaning solution is mixed and the mixture.

(h) Records are made of rejected materials being removed (by cutting) from sound material. The Inspection Department requests this work.

All cleaning solutions and rinse waters are sampled once daily and a sample log is maintained. The solutions are analyzed for chloride, fluoride, PH, phosphate, etc.

The TSP solution is dumped twice weekly unless the analysis indicates it should be discarded sooner. Solution is to be discarded if chloride is 10 ppm or more. The circulated hot rinse water is dumped twice daily.

Oxide Removal from Columbium-1% Zirconium and Tantalum Parts Prior to Welding

1. All oxide shall be removed by etching in a solution of:

   35% H_2SO_4
   15% HNO_3 (70% concentration) nitric acid
   10% HF (48% concentration) hydrofluoric acid
   40% distilled water

   The etching should be started in a solution at room temperature, and the solution temperature should not be allowed to exceed 125°F.

2. Prior to etching, each part shall be thoroughly degreased by wiping with acetone or ethyl alcohol.

3. Etching time in solution shall be determined by the thickness of the parts to be etched. Shimstock (.004 to .010 inch) material shall be etched for approximately 20 seconds.

4. All parts should be totally immersed in the solution and should be agitated to insure access of fresh solution to all surfaces. Particular care should be taken to assure the inner surfaces of tubing have access to fresh solution.

5. The parts shall be rinsed with distilled water at 125°F, or above, immediately upon removal from etching solution. Copious quantities of flowing distilled water shall be used to insure thorough rinsing. The parts shall be agitated during the rinse. A minimum of 30 minutes rinse shall be used. Particular care should be taken to assure that the inner surfaces of tubing have been rinsed. Parts shall not be allowed to dry during the transfer from etching solution to the distilled H_2O rinse.
6. Parts shall be thoroughly rinsed with acetone.
7. Parts shall be thoroughly rinsed with ethyl alcohol, drain dried, and placed in sealed polyethylene bags for storage.
8. Parts shall not be removed from storage bags until immediately prior to assembly.
9. Clean white gloves shall be worn when handling materials after Step 7.

Materials and Cleanliness Specification

A. All parts to be inside the vacuum system shall:
   1. Be identified as to type of material.
   2. Have a clean smooth surface equivalent to No. 16 finish, free of crevices, cracks, and/or other hard-to-clean areas.
   3. Be assembled so as to avoid the creation of closed or nearly closed volumes.
   4. Be cleaned according to the following procedure:
      a. Wash thoroughly with acetone.
      b. Wash with alcohol.
      c. Inspect the parts for visual evidence of remaining contamination, repeat (a) and (b), if required, to remove all contamination.
      d. Rinse with distilled water.
      e. Air dry in still air or use a warm air dryer; do not use plant air as it may be contaminated.
      f. Clean parts shall not be touched with bare hands, or placed on benches or in containers not thoroughly cleaned.
      g. Wrap or bag in polyethylene bags.

B. Workers shall wear the following clothing during cleaning and assembly of the system components;
   1. A pair of clean, white nylon or rayon acetate gloves.
   2. Clean dry coveralls or laboratory coats.
   3. Clean shoe covers if feet are inside the vacuum area or above the main vacuum tank flange and in the clean room. The above clothing must be changed whenever it becomes soiled.

C. Workers shall not smoke or chew tobacco while working in the clean room or vacuum tank area.

D. Tools used in assembly operations must be cleaned by the procedure outlined in A-4, or provided with clean covers so as to avoid any possible contamination.

E. Any discoloration or other evidence of contamination on parts to be used in the vacuum system shall be reported immediately to the Project Engineer.

F. Questions on this procedure or exceptions to it must be referred to the Project Engineer.

Definitions

1. Clean - free of all contaminants.
2. Contaminants - oil, grease, solvents, discoloration, fingerprints, dust, dirt, ink, or other markings not scratched, etched, or stamped into the metal, etc.
3. Vacuum Tank Area - within ten feet of the vacuum tank or within five feet of any components awaiting assembly.

Responsibility

A. Materials certification shall be ascertained from the Inspection Engineering Department.

B. Welding inspectors and shop foreman shall be responsible for determining that material certifications are available and that assembly personnel are equipped with clothing as specified above.

C. Final fabrication and assembly areas shall be approved by the project engineer. It is the intent that all assembled parts be cleaned prior to final installation in the vacuum chamber. Field fabrication and assembly shall be kept to a minimum.

ORNL-TM-2732

Internal Distribution

1. S. E. Beall
2. E. J. Breeding
3. Wm. B. Cottrell
4. F. L. Culler
5. B. Fleischer
6. A. P. Fraas
7. E. A. Franco-Ferreira (Y-12)
8. L. C. Fuller
9-11. P. A. Gnadt
12. W. R. Grimes
13. A. G. Grindell
14. W. O. Harms
15. P. N. Haubenreich
16. W. R. Huntley
17. P. R. Kasten
18. M. I. Lundin
19. R. N. Lyon
20. R. E. MacPherson
21. H. C. McCurdy
22. A. J. Miller
23. A. M. Perry
24. M. W. Rosenthal
25. A. W. Savolainen
26. J. H. Shaffer
27. M. J. Skinner
28. I. Spiewak
29. D. A. Sundberg
30. D. B. Trauger
31. G. D. Whitman
32-33. Central Research Library
34-35. Y-12 Document Reference Section
36-38. Laboratory Records Department
39. Laboratory Records Department (LRD-RC)

External Distribution

NASA Lewis Research Center, 21000 Brookpark Road, Cleveland, Ohio 44135:

40-61. H. M. Cameron, Mail Stop 500-201
D. G. Beremand, Mail Stop 500-201
H. O. Slone, Mail Stop 500-201
D. R. Packe, Mail Stop 500-201
P. A. Thollot, Mail Stop 500-201
W. T. Wintucky, Mail Stop 500-201
R. E. English, Mail Stop 500-201
J. N. Deyo, Mail Stop 500-201
R. L. Davies, Mail Stop 500-201
Herman Schwartz, Mail Stop 500-201
M. Gutstein, Mail Stop 500-201
B. Lubarsky, Mail Stop 3-3
N. T. Musial, Mail Stop 501-3
V. F. Hlavin, Mail Stop 3-14
W. Russell, Mail Stop 14-1
J. E. Dilley, Mail Stop 500-201
P. E. Foster, Mail Stop 3-19
Library, Mail Stop 60-3
Report Control Office, Mail Stop 5-5
Fluid System Components Div., Mail Stop 5-3
Reliability & Quality Assurance Office, Mail Stop 500-203

62. J. C. Nettles, Mail Stop 1441-1, NASA Lewis Research Center, Plum Brook Station, Taylor Road, Sandusky, Ohio 44870
63. H. D. Rochen, Code RNP, National Aeronautics & Space Adm., Washington, D. C. 20545

64. Arvin Smith, Code RNW, National Aeronautics & Space Adm., Washington, D. C. 20545
65. Acquisitions Branch (SQT-34054), NASA Scientific & Technical Information Facility, P. O. Box 5700, Bethesda, Maryland 20014
66. Library, NASA Ames Research Center, Moffett Field, California 94035
67. Library, NASA Goddard Space Flight Center, Greenbelt, Maryland 20771
68. Library, NASA Spacecraft Center, Houston, Texas 77058
69. Library, NASA Marshall Space Flight Center, Huntsville, Alabama 35812
70. W. Crim, U.S. Army Engineer R&D Labs, Gas Turbine Test Facility, Fort Belvoir, Virginia 22060
71. Library, Hughes Aircraft Corporation, Centinda & Teale Ave., Culver City, California 90230
72. Library, Air Force Systems Command, Aeronautical Systems Division, Wright-Patterson Air Force Base, Ohio 45433
73. Power Information Center, University of Pennsylvania, 3401 Market Street, Rm. 2107, Philadelphia, Pennsylvania 19104
74. Library, AiResearch Manufacturing Co., 402 South 36 Street, Phoenix, Arizona 85034
75. Lyle Six, AiResearch Manufacturing Co., 402 South 36 Street, Phoenix, Arizona 85034
76. NASA Flight Research Center, P. O. Box 273, Edwards, California 93523
77. NASA Langley Research Center, Langley Station, Hampton, Virginia 23365
78. Tony Redding, NASA Manned Spacecraft Center, Houston, Texas 77058
79. Library, Jet Propulsion Laboratory, 4800 Oak Grove Drive, Pasadena, California 91103
80. Library, Battelle Memorial Institute, 505 King Avenue, Columbus, Ohio 43201
81. Code RAPP, Bureau of Naval Weapons, Department of the Navy, Washington, D. C. 20025
82. Library, Institute for Defense Analyses, 400 Army-Navy Drive, Arlington, Virginia 22202
83. Library, Aerojet-General Corporation, Von Karman Center, Azusa, California 91702
84. H. Milligan, AiResearch Manufacturing Company, 402 South 36 Street, Phoenix, Arizona 85034
85. AiResearch Manufacturing Company, 9851 Sepulveda Boulevard, Los Angeles, California 90009
86. Library, Bendix Research Labs. Division, Detroit, Michigan 48232
87. Library, The Boeing Company, Aero-Space Division, Box 3707, Seattle, Washington 98124
88. Library, Continental Aviation & Engr. Corp., 12700 Kercheval Avenue, Detroit, Michigan 48215
89. Library, Curtiss-Wright Corporation, Wright Aero Division, Main & Passaic Streets, Woodridge, New Jersey 07075

90. Library, General Dynamics Corporation, 16501 Brookpark Road, Cleveland, Ohio 44142
91. Library, Aerospace Corporation, P. O. Box 95085, Los Angeles, California 91745
92. Library, General Electric Company, Missile & Space Vehicle Department, 3198 Chestnut Street, Philadelphia, Pennsylvania 19104
93. Library, Lear Siegler, Inc., 3171 S. Bundy Drive, Santa Monica, California 90406
94. Library, Massachusetts Institute of Technology, Cambridge, Massachusetts 02139
95. Library, Space Systems Division, Los Angeles Air Force Station, Los Angeles, California 90045
96. Library, Borg-Warner Corporation, Pesco Products Division, 24700 North Miles Road, Bedford, Ohio 44014
97. Library, Douglas Aircraft Company, 3000 Ocean Park Blvd., Santa Monica, California 90406
98. Library, General Electric Company, Mechanical Technology Laboratory, R & D Center, Schenectady, New York 12301
99. Library, General Electric Company, Flight Propulsion Division, Cincinnati, Ohio 45215
100. Library, McDonnell Douglas Corporation, Missile & Space Systems Division, 3000 Ocean Park Blvd., Santa Monica, California 90406
101. Library, General Motors Corporation, Indianapolis, Indiana 46206
102. Library, Lockheed Missiles & Space Co., P. O. Box 504, Sunnyvale, California 94088
103. Mechanical Technology, Inc., 968 Albany-Shaker Road, Latham, New York 12110
104. Library, North American Aviation, Inc., Space & Information Systems Div., Downey, California 90241
105. Library, Pratt & Whitney Aircraft, 400 Main Street, East Hartford, Connecticut 06108
106. Library, Solar, Div. of International Harvester, 2200 Pacific Highway, San Diego, California 92112
107. Library, Sunstrand Denver, 2480 West 70 Avenue, Denever, Colorado 80221
108. Library, United Aircraft Research Lab., East Hartford, Connecticut 06108
109. Library, Westinghouse Electric Corp., Astronuclear Laboratory, P. O. Box 10864, Pittsburgh, Pennsylvania 15236
110-111. R. W. Harrison, Gneral Electric Company, Nuclear Systems Programs, Cincinnati, Ohio 45215
112. I. Mendelson, General Electric Company, Nuclear Systems Programs, Cincinnati, Ohio 45215
113. Library, Northern Research & Engineering Co., 219 Vassar Street, Cambridge, Massachusetts 02139
114. Library, McDonnell-Douglas Corporation, Lambert Field, St. Louis, Missouri 63166
115. Library, Space Technology Labs. Inc., One Space Park, Redondo Beach, California 90278

116. Library, TRW Accessories Division, 23555 Euclid Avenue, Cleveland, Ohio 44117
117. Library, Williams Research, Walled Lake, Michigan 48088
118. J. Mattavi, General Motors Technical Center, Warren, Michigan 48089
119. A. Miklos, General Motors Technical Center, Warren, Michigan 48089
120-134. Division of Technical Information Extension (DTIE)
135. Laboratory and University Division, ORO